

The SAD-1 Kinase Regulates Presynaptic Vesicle Clustering and Axon Termination

Justin Gage Crump,* Mei Zhen,† Yishi Jin,†
and Cornelia I. Bargmann*‡

*Departments of Anatomy and
of Biochemistry and Biophysics
Howard Hughes Medical Institute
University of California, San Francisco
San Francisco, California 94143

†Department of Biology
Sinsheimer Laboratories
University of California, Santa Cruz
Santa Cruz, California 95064

Summary

During synapse formation, presynaptic axon outgrowth is terminated, presynaptic clusters of vesicles are associated with active zone proteins, and active zones are aligned with postsynaptic neurotransmitter receptors. We report here the identification of a novel serine/threonine kinase, SAD-1, that regulates several aspects of presynaptic differentiation in *C. elegans*. In *sad-1* mutant animals presynaptic vesicle clusters in sensory neurons and motor neurons are diffuse and disorganized. Sensory axons fail to terminate in *sad-1* mutants, whereas overexpression of SAD-1 causes sensory axons to terminate prematurely. SAD-1 protein is expressed in the nervous system and localizes to synapse-rich regions of the axons. SAD-1 is related to PAR-1, a kinase that regulates cell polarity during asymmetric cell division. Overexpression of SAD-1 causes mislocalization of vesicle proteins to dendrites, suggesting that *sad-1* affects axonal-dendritic polarity as well as synaptic development.

Introduction

The assembly of the nervous system occurs when neurons recognize appropriate targets and form electrical and chemical synapses with them. The signals that organize synaptogenesis are best characterized at the mammalian neuromuscular junction (NMJ) (reviewed in Sanes and Lichtman, 1999). During neuronal development, motor axons are precisely guided to the muscles they will innervate. Upon the axon's arrival at a target muscle, signals between the neuron and muscle induce cytoskeletal changes in the axonal growth cone, the clustering of neurotransmitter-filled vesicles and exocytotic machinery at presynaptic active zones, the postsynaptic aggregation of neurotransmitter receptors and regulatory proteins, and the formation of a stable adhesion between the neuron and muscle. The neuron secretes the extracellular matrix molecule agrin, which signals through the MuSK tyrosine kinase receptor to cluster acetylcholine receptors (Glass et al., 1996; Gautam et al., 1996; DeChiara et al., 1996). Mice deficient

in agrin or MuSK have defects in muscle differentiation and also have presynaptic defects in vesicle aggregation and axon termination, suggesting that the muscle sends a retrograde signal to the neuron to induce presynaptic differentiation. One candidate for a retrograde signal is laminin β 2, a component of the synaptic basal lamina. Laminin β 2 inhibits neurite outgrowth of cultured neurons (Porter et al., 1995), and mice lacking laminin β 2 have defects in presynaptic differentiation (Noakes et al., 1995). The receptors and signaling pathways that act downstream of laminin β 2 are unknown.

Although many of the principles governing NMJ synapse development probably apply to synapses between neurons, less is known about the molecules that regulate connectivity in the central nervous system (CNS). Two classes of transmembrane proteins, the neuroligin-neurexin complex (Butz et al., 1998; Scheiffele et al., 2000) and cadherins (Kohmura et al., 1998; reviewed in Shapiro and Colman, 1999), have been implicated in neuron to neuron adhesion at the initiation of CNS synapse formation. Synapses between neurons appear largely intact in agrin mutants (Serpinskaya et al., 1999). The secreted protein Wnt7A causes axonal remodeling and the accumulation of synapsin in cultured mossy fiber neurons; in *Wnt7A* mutants the presynaptic differentiation of mossy fiber granule cell synapses is delayed (Hall et al., 2000). In response to these or other factors, CNS neurons localize scaffold proteins at active zones, cluster vesicles nearby in a specialized cytoskeleton, and cease axon outgrowth. The signaling pathways that mediate these processes are undefined.

Several presynaptic proteins may serve as either regulators or targets of signals for presynaptic differentiation. Synapsins are lipid binding proteins that associate with synaptic vesicles (Hosaka et al., 1999) and have been implicated in their clustering at synaptic sites (Lu et al., 1992). A mouse synapsin I/synapsin II double knockout has a 50% reduction in the number of clustered synaptic vesicles (Rosahl et al., 1995). In *C. elegans*, the liprin protein SYD-2 controls the size of presynaptic specializations; in *syd-2* mutant animals active zones and vesicle clusters are expanded (Zhen and Jin, 1999). A vertebrate liprin interacts with tyrosine phosphatase receptors (Serra-Pagés et al., 1995). Three large proteins, Piccolo, Bassoon, and RPM-1/Highwire, localize at or near presynaptic specializations (tom Dieck et al., 1998; Fenster et al., 2000). Mutations in *C. elegans rpm-1* (Zhen et al., 2000; Schaefer et al., 2000) and its *Drosophila* homolog *Highwire* (Wan et al., 2000) lead to a variety of presynaptic structural defects depending on the type of synapse studied. These defects include reduced or disorganized presynaptic structures in *C. elegans* and hyperproliferation of synapses in *Drosophila*.

To identify novel regulators of presynaptic development we conducted direct visual screens in *C. elegans* for mutations that affect presynaptic vesicle clusters in the ASI chemosensory neurons. We describe the identification of a mutant, *sad-1*, that affects the presynaptic development of ASI and motor neurons. *sad-1* encodes

‡To whom correspondence should be addressed (e-mail: cori@itsa.ucsf.edu).

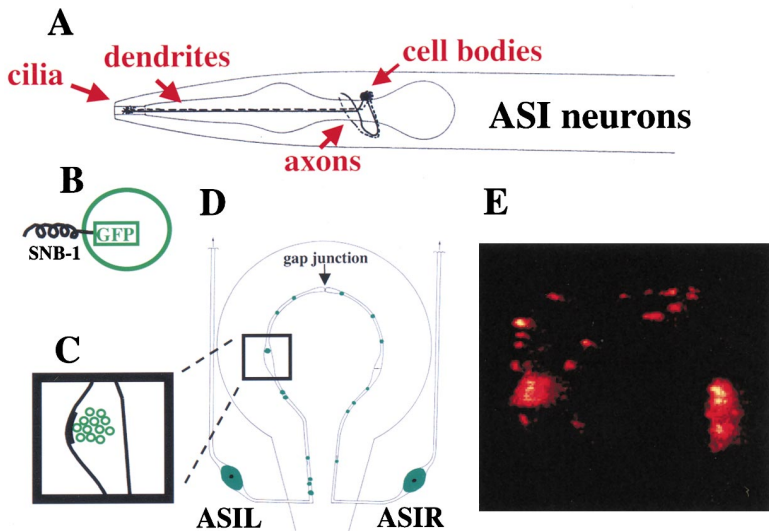


Figure 1. p_{str-3} SNB-1::GFP Labels Presynaptic Vesicle Clusters in the ASI Chemosensory Neurons

(A) Each ASI neuron sends a dendrite to the tip of the nose, where it ends in a cilium, and an axon into the nerve ring. The outline of the pharynx is diagrammed as a landmark. Anterior is left; dorsal is up. (B) A SNB-1::GFP fusion localizes GFP to the luminal side of synaptic vesicles. (C) Diagram of a typical synapse, with vesicles and an active zone in a slight thickening. (D) Flattened cross-section showing the predicted presynaptic specializations of the ASI neurons (adapted from White et al., 1986). The two larger shaded ovals are the cell bodies of ASIL and ASIR. The axons of ASIL and ASIR form gap junctions at their dorsal ends. The smaller shaded circles within the axons represent clusters of synaptic vesicles (see Figure 1C). (E) When expressed under the control of the ASI-specific *str-3* promoter, SNB-1::GFP allows the visualization of ASI presynaptic vesicle clusters in living animals.

The confocal epifluorescence micrograph is in roughly the same orientation as (D) with dorsal up and anterior into the page. The large fluorescent regions are the ASI cell bodies. The smaller puncta correspond well with the vesicle clusters diagrammed in (D).

a novel serine/threonine protein kinase that localizes to synapse-rich regions of the axon. In *sad-1* mutant animals presynaptic vesicle clusters are disorganized and sensory axons fail to terminate properly; conversely, when SAD-1 is overexpressed ectopic vesicle proteins appear in the dendrite and sensory axons terminate prematurely. Thus, SAD-1 appears to regulate several aspects of presynaptic differentiation.

Results

Isolation of Mutants with Defective Chemosensory Synapses

The ASI neurons are a bilaterally symmetric pair of chemosensory neurons that control entry into the dauer larva stage (Bargmann and Horvitz, 1991). Each ASI neuron has a ciliated dendrite that projects anteriorly and an axon that enters the nerve ring and makes seven to nine synapses onto interneurons and chemosensory neurons (White et al., 1986) (Figures 1A, 1C, and 1D). To visualize the presynaptic specializations of ASI synapses in living animals, we expressed a fusion protein between the vesicle associated membrane protein synaptobrevin and green fluorescent protein (SNB-1::GFP) under the control of the ASI neuron-specific *str-3* promoter (Figure 1B). SNB-1::GFP is an accurate marker for presynaptic vesicle clusters in *C. elegans* (Nonet, 1999). In each ASI neuron of animals carrying p_{str-3} SNB-1::GFP, GFP fluorescence was visible in seven to nine regularly spaced clusters along the distal half of the axon in the nerve ring (Figures 1, 2A, and 2B). The clusters observed in each ASI neuron corresponded well with the ASI synapses observed in electron microscopic reconstructions (White et al., 1986) (compare Figures 1D and 1E). GFP was also present in the cell body and weaker, diffuse fluorescence was occasionally observed in the dendrite. To confirm that the axonal SNB-1::GFP fluorescence corresponded to presynaptic vesicles, we examined p_{str-3} SNB-1::GFP in the *unc-104*

kinesin mutant. In *unc-104* mutant animals synaptic vesicles accumulate in the cell body and are largely absent from the axon (Otsuka et al., 1991). As expected for a marker of synaptic vesicles, p_{str-3} SNB-1::GFP fluorescence accumulated in the cell body in *unc-104(e1265)* mutant animals (data not shown).

Using p_{str-3} SNB-1::GFP as a marker for ASI synapses, we conducted a screen for mutants with abnormal patterns of GFP fluorescence. Hermaphrodites carrying p_{str-3} SNB-1::GFP were mutagenized with EMS, and their F2 progeny were examined for visible defects (see Experimental Procedures). We isolated 24 mutations in six complementation groups that affect the pattern of SNB-1::GFP expression: *unc-104*, *unc-11*, *unc-51*, and three novel genes that we named *sad-1*, *sad-2*, and *sad-3* for synapses of the amphid defective (Table 1). [In Zhen et al. (2000), we report that *sad-3* is allelic with *rpm-1*.] Multiple alleles were identified in each of these genes, suggesting that this visual screen is near genetic saturation.

The three *unc* genes isolated in this screen all affect synaptic vesicle biogenesis or transport. As expected from our analysis of *unc-104(e1265)*, the novel *unc-104* kinesin mutants had SNB-1::GFP localized to the cell body (data not shown). In *unc-11* animals GFP fluorescence was diffusely localized throughout the plasma membrane of the neuron (described in more detail in Dwyer et al., submitted). *unc-11* is an AP180 protein implicated in synaptic vesicle endocytosis that is essential for SNB-1 localization to vesicles (Nonet et al., 1999). In *unc-51* animals GFP fluorescence accumulates in one or two large varicosities in the axon (data not shown). *unc-51* encodes a protein kinase that affects axon outgrowth and guidance and may alter trafficking of membrane vesicles in neurons (Ogura et al., 1994). We isolated both strong and weak *unc-51* alleles that affect synaptic vesicle clusters but not axon guidance in ASI. *unc-51* is similar to the Apg1p kinase that acts at an early step in yeast autophagy (Matsuura et al., 1997). By analogy to the yeast phenotype, *unc-51* may be in-

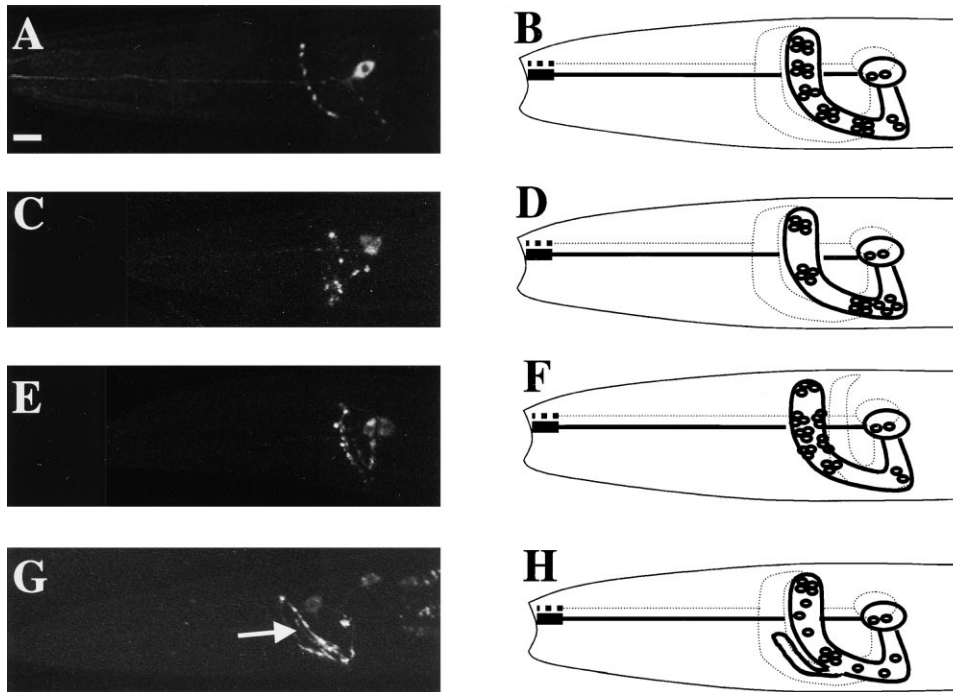


Figure 2. In *sad-1* Mutants SNB-1::GFP Clusters Are Disorganized and More Diffuse in the ASI Neurons

Confocal epifluorescence micrographs (A, C, E, G) and interpretive diagrams (B, D, F, H) of p_{str-3} SNB-1::GFP expression in wild-type (A, B) and *sad-1(ky330)* (C–H) animals. In wild-type animals, SNB-1::GFP clusters were regularly spaced along the ASI axon (A, B). In *sad-1(ky330)* animals clusters were absent in regions of the axon (C, D), uneven in size, and spatially disorganized (E, F) or diffuse (G, H). The arrow in (G) denotes a secondary branch emanating from the primary axon. In (G) and to a lesser extent in (A, C, E) the axon of the contralateral ASI neuron is faintly visible (designated by dotted lines in diagram).

involved in the budding of synaptic vesicles from endosomes or other internal membrane compartments.

sad-1 Mutants Have an Altered Distribution of Synaptic Vesicles

Whereas mutations in *unc-104*, *unc-11*, and *unc-51* have effects on trafficking of vesicles and/or synaptobrevin, mutations in *sad-1*, *sad-2*, and *sad-3/rpm-1* have defects in the organization of SNB-1::GFP clusters. We isolated six alleles (*ky281*, *ky289*, *ky326*, *ky330*, *ky332*, and *ky344*) of *sad-1* in the p_{str-3} SNB-1::GFP screen, and a seventh allele (*ju53*) in a similar type of screen using p_{unc-25} SNB-1::GFP (see below). All alleles displayed highly penetrant SNB-1::GFP defects in ASI, with over 90% of animals exhibiting a visible defect. The spectrum of defects included regions of the axon that appeared to lack vesicle clusters (Figures 2C and 2D); regions of the axon with densely packed vesicle clusters (Figures 2E and 2F); vesicle clusters that were irregular in size,

often appearing smaller than normal (Figures 2E and 2F and data not shown); and axons that displayed diffuse SNB-1::GFP fluorescence (Figures 2G and 2H). The phenotypes of most animals represented a combination of these defects.

sad-1 mutants also have presynaptic defects at neuromuscular junctions. p_{unc-25} SNB-1::GFP labels the presynaptic vesicle clusters of the GABAergic VD and DD motor neurons (Hallam and Jin, 1998). In wild-type animals this marker is expressed as discrete fluorescent puncta distributed along the ventral and dorsal sides (Figure 3A). The *ju53* allele of *sad-1* was isolated as a mutant in which SNB-1::GFP clusters appeared less discrete (Figures 3B to 3D), with weaker GFP fluorescence than normal. Similar VD and DD defects were observed for the *ky289*, *ky330*, and *ky332* alleles. All (100%) of *sad-1* mutants had visible VD and DD defects, and >75% of individual puncta were expanded compared to wild-type puncta. However, the total number of puncta is normal: the dorsal cord in *sad-1(ju53)* has 148.6 SNB-1::GFP puncta ($n = 5$, range 145–153), compared to the wild type with 150 ± 5 puncta.

In the first larval stage (L1) the DD motor neurons have both ventral and dorsal processes but make synapses exclusively onto ventral muscle. In *sad-1* mutants SNB-1::GFP was localized to both the ventral and dorsal processes of L1 DD motor neurons (data not shown). Either synaptic vesicles are not properly anchored at, or targeted to, synaptic regions or SAD-1 regulates the ventral-dorsal polarity of the DD neurons.

Table 1. A Genetic Screen for SNB-1::GFP Clustering Defects in the ASI Neurons

Gene	Alleles Isolated
<i>unc-104</i>	<i>ky287</i> , <i>ky290</i> , <i>ky317</i> , <i>ky319</i>
<i>unc-11</i>	<i>ky280</i> , <i>ky291</i> , <i>ky325</i>
<i>unc-51</i>	<i>ky286</i> , <i>ky321</i> , <i>ky322</i> , <i>ky323</i> , <i>ky324</i> , <i>ky347</i>
<i>sad-1</i>	<i>ky281</i> , <i>ky289</i> , <i>ky326</i> , <i>ky330</i> , <i>ky332</i> , <i>ky344</i>
<i>sad-2</i>	<i>ky292</i> , <i>ky329</i> , <i>ky335</i>
<i>sad-3/rpm-1</i>	<i>ky340</i> , <i>ky346</i>

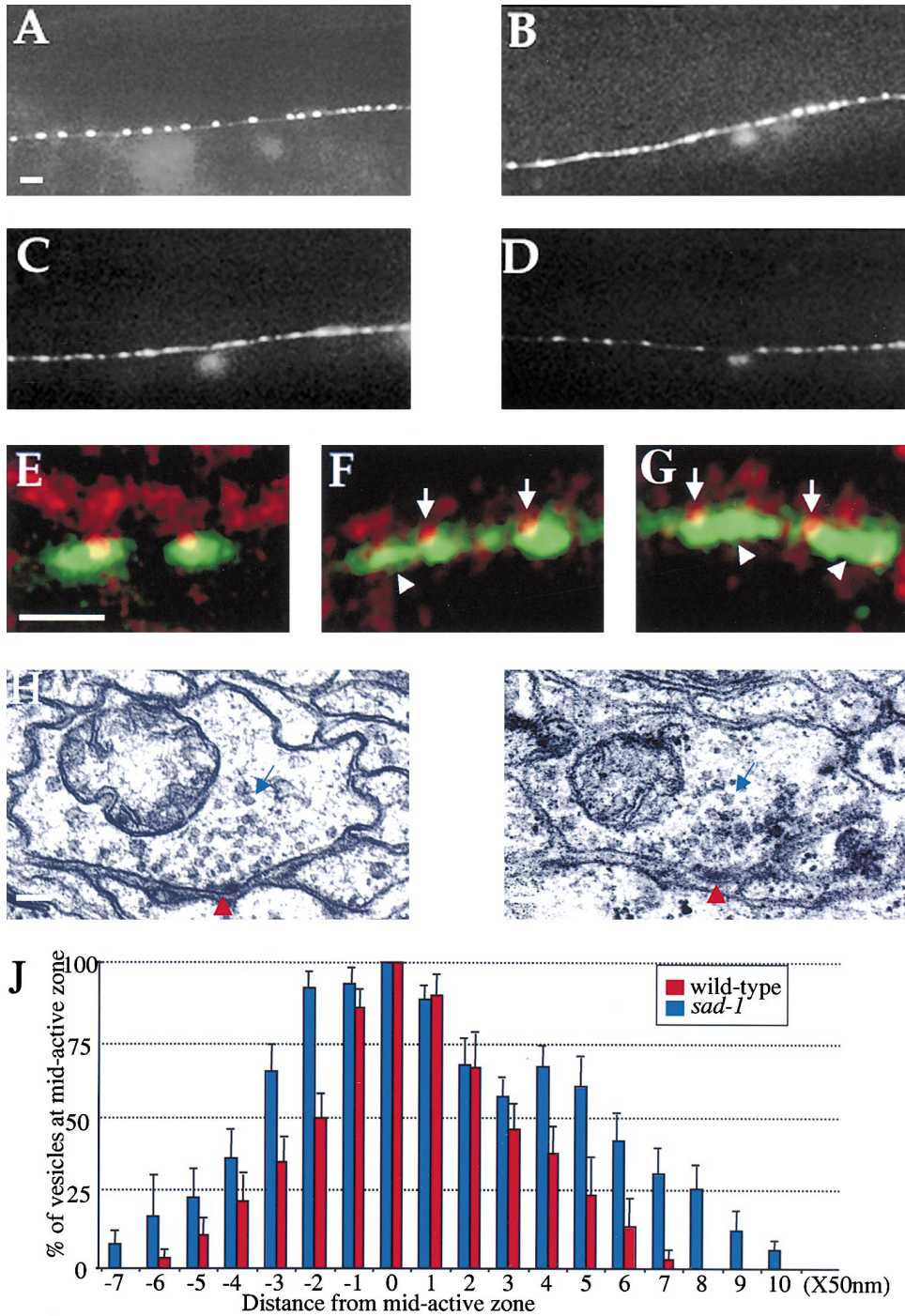


Figure 3. SNB-1::GFP Clusters, but Not SYD-2 Localization, Are Disrupted at the NMJ of *sad-1* Mutants

Fluorescence micrographs of wild-type (A) and *sad-1(ju53)* (B–D) animals expressing the p_{unc-25} SNB-1::GFP marker. p_{unc-25} SNB-1::GFP labels the presynaptic vesicle clusters of the GABAergic VD and DD motor neurons. In wild-type animals, SNB-1::GFP clusters are of uniform size and regularly spaced (A). In *sad-1(ju53)* mutants, these clusters appeared less discrete (B) or diffuse (C) and weaker in fluorescence (D). (E–G) show the expression of SYD-2 (red) and SNB-1::GFP (green) in wild-type (E) and *sad-1(ju53)* animals (F, G). SYD-2 localizes near or at presynaptic active zones. In wild-type animals, a single punctum of SYD-2 (red) is localized to the middle of SNB-1::GFP clusters (green) (E). In *sad-1(ju53)* animals, most SNB-1::GFP clusters were irregularly shaped (arrowheads), but SYD-2 puncta appeared normal (arrow) (F, G). Scale: 4 μ m. (H, I) Electron micrograph cross-sections of a GABAergic neuromuscular junction in a wild-type (H) and a *sad-1(ky289)* (I) animal. The active zone (red arrowheads), vesicles (blue arrows), and cytoskeleton of the presynaptic zone were normal in *sad-1* mutants. Scale bar: 140 nm. (J) Vesicle distribution is more diffuse in the GABAergic NMJs of *sad-1(ky289)* animals. The distribution of vesicles in 10 GABAergic synapses each of wild-type (N2, shown in red) and *sad-1(ky289)* (in blue) were analyzed in serial section electron micrographs. The vesicle number at the active zone was normalized to 100%, and the vesicle number at each succeeding 50 nm section was compared to that peak value. Wild-type and *sad-1* mutants were significantly different in vesicle distribution at $p < 0.05$.

In contrast to *unc-104*, *unc-11*, and *unc-51* animals, which displayed severely uncoordinated locomotion, *sad-1* animals had only subtle defects in movement. *sad-1* mutants were partially defective in chemotaxis to volatile odorants (data not shown) and had mild defects in egg-laying. In *sad-1* animals the ASI cell bodies migrated to their correct locations, and their primary axons assumed their normal position and morphology in the nerve ring. However, as discussed in more detail below, axons sometimes made ectopic branches in the nerve ring and failed to terminate at their normal position. To determine whether the ASI neurons are functional in *sad-1* mutants, we analyzed *unc-31; sad-1* double mutants. Ablation of the ASI neurons in an *unc-31* background causes animals to constitutively enter the alternative dauer larval form despite the presence of food (Avery et al., 1993). This activity of ASI depends on its ability to secrete the TGF- β -like peptide DAF-7 (Ren et al., 1996; Schackwitz et al., 1996). DAF-7 is most likely released from dark-core vesicles at extrasynaptic sites (White et al., 1986). *unc-31; sad-1* animals formed almost no dauer larvae in the presence of food, suggesting that the ASI neurons are present in *sad-1* animals and able to release DAF-7.

SYD-2, a Presynaptic Marker for Active Zones, Is Correctly Localized in *sad-1* Mutants

To characterize the presynaptic defects in *sad-1* animals further, we examined a presynaptic active zone marker, SYD-2. SYD-2 localizes to small regions at presynaptic termini that are surrounded by SNB-1::GFP vesicle clusters (Zhen and Jin, 1999 and Figure 3E). In wild-type animals anti-SYD-2 staining reveals a dense pattern of puncta in the nerve ring; on a gross level we noticed no major differences in this staining between wild-type and *sad-1* animals (data not shown). To examine individual synapses at higher resolution, we visualized SYD-2 and SNB-1 specifically in the VD and DD neurons in a *sad-1* mutant background. Using the *unc-25* promoter we coexpressed SYD-2 and SNB-1::GFP in the VD and DD motor neurons in a *syd-2(ju37) sad-1(ju53)* double mutant and stained with anti-SYD-2 and anti-GFP antisera. P_{unc-25} SYD-2 fully rescued the *syd-2* mutant phenotype in VD and DD neurons (Figure 3E). In the *sad-1* mutant, the expression pattern of SYD-2 appeared normal (Figures 3F and 3G). Each SYD-2 punctum was associated with a vesicle cluster and vice versa; since the number of vesicle clusters is normal (see above), we infer that the number of SYD-2 puncta is also normal. As expected from examining SNB-1::GFP alone, the SNB-1::GFP clusters associated with SYD-2 puncta were abnormally diffuse. We conclude that SAD-1 is not required for at least some aspects of active zone formation. Consistent with this observation, *syd-2(ju37) sad-1(ju53)* double mutants showed more severe defects in SNB-1::GFP organization than either single mutant (data not shown). This result suggests that *sad-1* and *syd-2* function in different aspects of synaptic development.

Synaptic Vesicles Are More Broadly Distributed at GABAergic Neuromuscular Junctions in *sad-1* Mutants

The diffuse localization of the SNB-1::GFP marker suggested that synaptic vesicle distribution was altered in

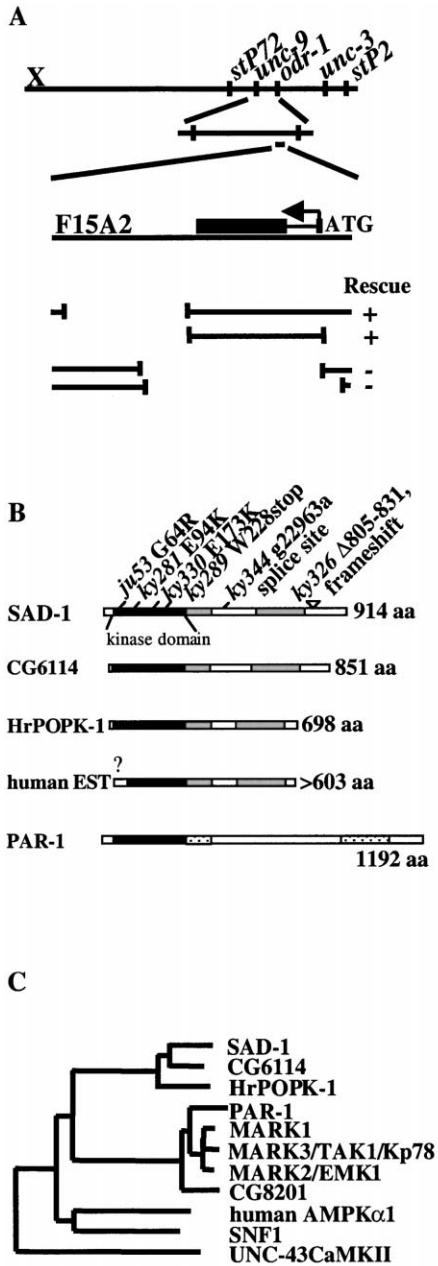
sad-1 mutants. To strengthen this observation, we performed electron microscopic analysis on the VD neuromuscular junctions in *sad-1(ky289)* animals (Figures 3H to 3J). The presynaptic structures in VD neuromuscular junctions were superficially normal. Each presynaptic terminal contained an electron-dense membrane structure, the active zone, that was indistinguishable from the active zone in wild-type animals (Figures 3H and 3I). The cytoskeleton and overall structure of the axons was normal.

As in wild-type presynaptic termini, the active zones in *sad-1* mutants were surrounded by synaptic vesicles. The vesicle morphology was normal, and a normal number of vesicles were docked at the active zone. However, the vesicles in *sad-1* mutants were distributed more broadly around the synapse. We analyzed the distribution of vesicles by taking serial sections through ten presynaptic termini each for wild-type and *sad-1* mutant and counting the number of vesicles in each section (Figure 3J). Three statistically significant differences were observed ($p < 0.05$). First, in wild-type animals, vesicles are highly concentrated so that >100 nm from the active zone, wild-type synapses had less than 50% as many vesicles as were present at the active zone. A comparable drop in vesicle density occurred 150–250 nm from the *sad-1* active zone. Second, the average size of wild-type GABAergic presynaptic termini, defined as the region where synaptic vesicles can be counted, was 700 nm (14 sections). In *sad-1(ky289)* animals, the region was expanded to 900 nm (18 sections). Third, for 6/10 *sad-1* synapses, there was an overlap between the vesicles distributed at two adjacent synapses; such overlaps were observed at only 5/33 wild-type synapses. Overlapping synapses were excluded from the analysis of synapse size, so the 900 nm total size underestimates the expanded vesicle distributions of the *sad-1* mutant. Thus, as suggested by the SNB-1::GFP pattern, synaptic vesicles are distributed more diffusely in the GABAergic presynaptic termini of *sad-1(ky289)* animals.

SAD-1 Protein Is a Novel Serine/Threonine Kinase

sad-1 was cloned by genetic mapping and cosmid rescue of its mutant phenotype. The cosmid F15A2 fully rescued the ASI defects of *sad-1(ky332)* and partially rescued the VD/DD SNB-1::GFP defects of *sad-1(ju53)*. A fragment of F15A2 that contained only a single predicted full-length open reading frame (ORF) also rescued *sad-1* to the same degree as the full-length cosmid, whereas fragments of F15A2 not containing this ORF failed to rescue (Figure 4A). We obtained a partial cDNA corresponding to this ORF (a gift of Yuji Kohara) and performed reverse transcriptase-polymerase chain reaction (RT-PCR) to clone the 5' end of the gene. The major full-length cDNA is predicted to encode a protein of 914 amino acids. All exons and intron/exon boundaries were sequenced in the seven *sad-1* alleles and molecular lesions were identified in six (Figure 4B). We conclude that mutations in this ORF are responsible for the *sad-1* phenotype.

sad-1 encodes a novel protein predicted to encode a serine/threonine kinase. There are highly conserved homologs of *sad-1* in *Drosophila*, the ascidian *Halocynthia roretzi*, and humans, but the functions of these homologs



D

Protein	Sequence
SAD-1	M F E A L K E V L G E I N S K L A A V N N E L S S K I M S E N I V S T R P V A Q A D V C R P Y K L E
CG6114	M Q K E N N V T A E N C S V G P Y R L E
HrPOPK-1	M S N A P G P G Q V Y G P Y K L E
PAR-1 (kinase domain)	V G R Y K L L
SAD-1	K T L G K G Q T G L V K L G V H C I Y G R K V A I K I V N K E K L S E S V L O K V E R E I A I M K L
CG6114	K T L G K G Q T G L V K L G V H C V I G K K V A I K I I N R E K L S E S V L O K V E R E I A I M K L
HrPOPK-1	K T L G K G Q T G L V K L G V H C M T G K K V A V K I V N R E K L S E S V I N K V E R E I A I M K L
PAR-1	K T I G K G N F A K V K L A K H V I T G H E V A I K I I D K T A L N P S L E O K L F R E V R I M K L
SAD-1	E H P N V L H V D V Y E N K K Y L Y L L E H V S G G E L F D Y L V R K R R L M Q K E A R K F F
CG6114	I D H P H V L G L S D V Y E N K K Y L Y L I L E H V S G G E L F D Y L V K K G R R L T P K E A R K F F
HrPOPK-1	E H P H I L G L H D V Y E N K K Y L Y L I L E V S G G E L F D Y L V K G R R L T P R E A R R F F
PAR-1	L D H P N I V K L Y G V F E T E C T L Y V L E V A S G G E V F D Y L V H G R M K E K E A R A K F
SAD-1	R Q I I S A L D F C H A H N I C H R D L K P E N L L D E R N N I K V A D F G M A S L G V E S S M L
CG6114	R Q I I S A L D F C H S H S I C H R D L K P E N L L D E K N N I K I A D F G M A S L G P A S S M L
HrPOPK-1	R Q I I S A V D Y C H N I H V C H R D L K P E N L L D E K N N I K V A D F G M A S L O P E S T L L
PAR-1	R Q I V S A V D I H S K N I I H R D L K A E N L L D D P M N I K I A D F G F S N T F S L G N K L
SAD-1	E T S C G S P H Y A C P E V I R G E K Y D G R K A D V W S C G V I L Y A L L V G A L F F D D N L R
CG6114	E T S C G S P H Y A C P E V I R G E K Y D G R K A D V W S C G V I L Y A L L V G A L F F D D N L R
HrPOPK-1	E T S C G S P H Y A C P E V I R G E R Y D G R T A D V W S C G V I L F A L L V G A L F F D D N L R
PAR-1	D T F C G S P H Y A A P E L F S G R K Y G P E V I D V W S C G V I L Y L T L V G S L P F D G L N L A
SAD-1	N L L E K V K R Q V F H I P H F V P P D Q S L L R G M I E V N P O R R L T I A E I N R H P V W T A
CG6114	Q L L E K V K R Q V F H I P H F V P P D Q S L L R G M I E V N P O R R L T I A E I N R H P V W T A
HrPOPK-1	Q L L E K V K R Q V Y H I P H F V P P D A Q N L L R G M I D V R P D K R L S Q Q L L R H P W M R P
PAR-1	E L R E R V I R G K Y R I P F V M S T I D C E N L L K R F L V I N P Q R R S L D N I M K D P M M N V
SAD-1	T R A A P . . . E L E L P M S Q V V Q T H V I P G E D S I D P D V L R H N N C L G C F K D K R L
CG6114	G G K S L . . . E L L P M M E V V G T H V I P T A T V D P D V L N A C S L G G C F K E K E K L
HrPOPK-1	G S T V E G V L Y T P D P V F V I D C V P L E E S V D P D V L A S M T S L G C F K E K E K L
PAR-1	G Y E D E
SAD-1	N E L L S P K N T E K W V Y L L L D R K R R N A A Q E D D T E T V L T Q . . . A A G N N T P R
CG6114	I Q E L L S S N H T E K V I V F L L E R K R R R P A L E D D D E I J A Q K S R S E L D A V D P P R
HrPOPK-1	L R N L I T E G N T E K V V Y M L L R K K R Y P S F D D A D S L P . . . C K H P D P R
SAD-1	K R I T D S R T S R Y . . . P M G S I A D G S P L T N P K T Y G R N K S G R H S L G G S P T E S
CG6114	K R L D T C R I N G T N A P S Y G Q I S E G S P L T P R R Q A F N R S Y S T R N H Q S S P T T
HrPOPK-1	K R V P S T S L S S . . . S N G D D W C V N P P G
SAD-1	P R S T R D T F G S S S . . . G S Y S A R A G E D R D R G R S A S R
CG6114	S H T S S V S R L T R C N S P M S A Q Q Q A N A I S R P S S P A A G T R H S T Y G D R D R
HrPOPK-1	K M S A E S C L T D S . . . S P L S R K K S T E T H Q K G S L
SAD-1	S I N T Y H Y Y T Q V D P Q T L A E A A R H V R D A Q E R I R E S R D S G R G S S R K E S K R D R . .
CG6114	S H T S S V S R L T R C N S P M S A Q Q Q A N A I S R P S S P A A G T R H S T Y G D R D R
HrPOPK-1	T G E I N S R L V C N D Q T A E S K S R I N G T P R R D R G T C
SAD-1	S D K S A S S T C K N D A S T S S V F H K V S T P S V M S E S V V S S T M N S S T N S S T N S
CG6114	D C G I P P O S P G G N S S G S T S A S P S V I R A N S Q P T I A I I V N . . . P N G P M M N S
HrPOPK-1 S N O P V E I O I N T P A S P N
SAD-1	L I A G N S Q T S I G S T S G P W R S K L N N I K N S F L G T P R F H R R K M S N G T A E S D S E
CG6114	S P G M P S P C N T P G Q Q L W K T R L T N I K N S F L G S P R F H R R K M Q V A D E V H . . .
HrPOPK-1 P W R O R L A S L K N T F M G S P R F H R R K M G A P S S E D . . . V
SAD-1	D S Q M I D T I D L V K K S W F G S L A S S M S V E R D D T H C V P V Q G K T L N S T K A E
CG6114	L T P S S P L Y K R S W F G N I T T E K G S L . . . T F T I L V K G K P I A I T V K A I
HrPOPK-1	E N Q G N S S E L S K R S W F G N F M S S R Y S T E H C D E L F P Y A I A Y K N R I L N S Y K S E
SAD-1	I R A F L Q I T H E L S H S V V G Q N C H R V E Y K R . G P T V G S V F S R Q I T M N V D I P S
CG6114	L I H A F L S M A E L S H S V S P T S R F V E Y K R . . . N G N Q P V M F R H V K F Q V D I S A I
HrPOPK-1	L V H A F L S P N L T H S M V S P T R F R C D Y R S S T S T S V F T Q R S I K F Q V D I Q H
SAD-1	P Q . V V I A G E T P T V V I Q F V L A G P V R F R K R L V E H C S A I L I Q N S T O
CG6114	C K Q G D I A D M L F A L T F L L S G M I R R F R R I C V E H I Q S V C S K R F
HrPOPK-1	S S L D R Q E N G K P S S Q T V G S F T I A F S L I S G P I R R Y K R V E L L G M G M S I V A A
SAD-1	Q R A D R Q Q A A L M V R P R A L S D S S V G S A C S D S E S N A S S I N M I A R H S D K T E T T
CG6114	P G P S S P . . . P T V S V T Q A V S S S S C G S S S E R L S Y K R Q V I E N D M E N D S I F S
HrPOPK-1	N Q Q N K
SAD-1	S A T S S D P Y G P S M R S V G S G T A N S Y K S P T P H R R N T A V T A S S S A S N H Y G
CG6114	Y K S G N G R R A S T T N N N A N P V D T P G S P I A V R S S E T A E H E R N R E Q S E R R O A
HrPOPK-1 T S G E S A F S H E I Q L C K T V N L N H Q D N S T I A I N N P N
SAD-1	P S S S S G S G S S N N A D Y S Y H P E Y S Q R S N G S S A P K N O Y S P G S Q R S F A F S M F N K
CG6114	T T M S G S A I A
HrPOPK-1	H K S K V K
SAD-1	A D K V

Figure 4. SAD-1 Protein Is a Novel Serine/Threonine Kinase

(A) The *sad-1(ky332)* mutation was mapped near *odr-1* on the right arm of the X chromosome. A pool containing five cosmids rescued the ASI SNB-1::GFP defects of *sad-1(ky332)*. The cosmid F15A2 fully rescued the ASI SNB-1::GFP defects of *sad-1(ky332)* and partly rescued the VD/DD SNB-1::GFP defects of *sad-1(ju53)*. A SacII deletion version of F15A2 (first line) and a 13.8 kb fragment from F15A2 that contained a single predicted ORF (F15A2.6) (second line) also rescued *sad-1(ky332)*. Deleted versions of F15A2 not containing this ORF failed to rescue (third and fourth lines).

(B) A full-length cDNA corresponding to F15A2.6 predicts a 914 amino acid protein with homology to serine/threonine protein kinases. Mutations were found in the alleles *ju53*, *ky281*, *ky289*, *ky326*, *ky330*, and *ky344* [see text and (D)]. SAD-1 has homologs in *Drosophila* (CG6114), ascidians (HrPOPK-1), and humans (partial EST). The kinase domain of SAD-1 (aa 42–298) (black bars) is 85% identical to that of CG6114 and 82% identical to that of HrPOPK-1. SAD-1 and its homologs share conservation in two regions outside of the kinase domain (gray bars) [aa 301–400: 61% identity (CG6114), 43% identity (HrPOPK-1); aa 589–755: 44% identity (CG6114), 39% identity (HrPOPK-1)]. The kinase domains of

are unknown. The *H. roretzi* homolog, HrPOPK-1, was discovered in a search for mRNAs that localize to the posterior pole of the ascidian one-cell embryo (Sasakura et al., 1998); the *Drosophila* homolog was identified by genome project (Adams et al., 2000); and the human homolog is represented by an expressed sequence tag (EST) from an infant brain cDNA library. All four proteins share an N-terminal kinase domain (>82% identity) followed by a short conserved region, an unconserved linker, and a conserved 167 amino acid C-terminal domain (>39% identity) (Figure 4B).

The SAD-1 kinase domain shows homology to the AMPK/SNF1 family of serine/threonine kinases, with strongest similarity in *C. elegans* to PAR-1 (Guo and Kempthues, 1995). SAD-1 and PAR-1 share extensive similarity throughout their kinase domains (51% identity) but are not conserved outside this domain (Figures 4B and 4D). PAR-1 is related to a family of vertebrate kinases that includes MARK1, MARK2/EMK1, and MARK3/C-TAK1/Kp78 (Drewes et al., 1995) (Figures 4C and 4D).

The *sad-1* allele *ky289* contains an early nonsense mutation that truncates the predicted protein in the middle of the kinase domain. *ky289* likely represents the null phenotype of *sad-1*. *ky281* and *ky330* contain charge substitutions in highly conserved regions of the kinase domain; in particular, the *ky330* E173K mutation occurs four residues from the active site aspartate residue that is conserved in almost all known kinases. These point mutations suggest that the kinase activity of SAD-1 is essential for its function. The *ju53* allele is a glycine to arginine substitution in a less conserved region of the kinase domain. *ky344* and *ky326* encode proteins that retain an intact kinase domain but are missing C-terminal regions. *ky344* is a g22963a 5' splice site mutation at the border of intron 8 and exon 9 that is predicted to abolish splicing; the resulting protein would be effectively truncated after amino acid 475. *ky326* is a deletion of amino acids 805–831 that leads to a subsequent frameshift in the *sad-1* gene; the resulting protein would be effectively truncated at amino acid 805. The *ky344* and *ky326* mutations suggest that the C-terminal domains are also essential for SAD-1 function. An alternative explanation is that mutations in *ky344* and *ky326* affect the kinase domain indirectly by destabilizing *sad-1* mRNA. *C. elegans* transcripts containing premature stop codons are targeted for degradation by the products of the *smg* genes (Pulak and Anderson, 1993). The phenotype of *smg-3; sad-1(ky344)* animals was indistinguishable from that of *sad-1(ky344)* animals alone, suggesting that the protein itself is defective and not just the RNA (data not shown).

SAD-1 Is Expressed in Neurons and Localizes to Synapse-Rich Regions of Axons

To determine where *sad-1* was expressed, we used 5' regulatory elements from the *sad-1* locus to drive ex-

pression of GFP in transgenic animals. GFP was cloned in frame to the second exon of SAD-1 to create a protein fusion between the first 29 amino acids of SAD-1 and GFP (Figure 5A; this clone included 2 kb of upstream promoter sequences and the 6.6 kb first intron). In animals transgenic for p_{sad-1} GFP, fluorescence was seen in the entire nervous system beginning at late embryogenesis and continuing through adulthood (Figures 5B to 5D). We observed no expression in any tissues outside of the nervous system. Within neurons, GFP fluorescence was uniformly distributed, indicating that the small portion of SAD-1 protein fused to GFP did not localize to a particular subcellular region. To confirm the *sad-1* expression pattern suggested by p_{sad-1} GFP, we generated antibodies against a unique region of SAD-1. Only weak expression of SAD-1 was visible in wild-type animals, but in animals overexpressing SAD-1 from the endogenous promoter SAD-1 immunoreactivity was present throughout the nervous system (Figures 5E and 5G and data not shown). As with p_{sad-1} GFP, expression was first seen in the late embryo. We observed no consistent anti-SAD-1 staining in *sad-1(ky289)* null animals, suggesting that the antibodies are specific for SAD-1 protein. The onset of *sad-1* expression in the late embryo is consistent with a role for SAD-1 in synaptogenesis, as this is the time when many synapses are first made.

Since *sad-1* animals have specific defects in synaptic development, we asked whether SAD-1 protein localizes to synaptic regions. The pan-neuronal *unc-115* promoter (Lundquist et al., 1998) was used to express a SAD-1::GFP fusion protein in which GFP was inserted in the variable linker region that connects the N-terminal kinase domain with the conserved C-terminal domain (Figure 5I). Both wild-type SAD-1 and this GFP fusion caused paralysis and other phenotypes when expressed at high concentrations (discussed in more detail below), but at the lower concentrations examined in this experiment $p_{unc-115}$ SAD-1::GFP did not cause locomotion defects. SAD-1::GFP fluorescence was most prominent in the nerve ring and the ventral and dorsal cords, regions of the axon where the majority of synapses are made (Figure 5J). Little or no staining was observed in the sensory dendrites or the axonal commissures, which are devoid of synapses. Weaker fluorescence was also visible in the neuronal cell bodies excluded from the nucleus.

This general pattern of localization to synapses was confirmed by antibody staining of animals overexpressing SAD-1 from its own promoter. When SAD-1 localization was examined in animals that did not exhibit gain-of-function phenotypes (Figures 5E and 5F, and see below), SAD-1 expression was very similar to that of $p_{unc-115}$ SAD-1::GFP. Staining was present in synapse-rich regions of the nerve ring and nerve cords and in the cell bodies, but no staining was observed in the sensory dendrites or axonal commissures (Figure 5E). This result

SAD-1 and PAR-1 are 51% identical. Although SAD-1 and PAR-1 have a similar domain structure (stippled shading, regions conserved in all PAR-1-like proteins), they share no homology outside of the kinase domain.

(C) Dendrogram of the kinase domains of AMPK/SNF-1 family members and CaMKII. The SAD-1 group and PAR-1 group are more closely related to each other than to human AMPK α 1 and yeast SNF1.

(D) Alignment of SAD-1, CG6114, HrPOPK-1, and the PAR-1 kinase domain. Identical residues are boxed and shaded. Similar residues are boxed. Black bars denote the kinase domain. Gray bars denote regions of homology outside the kinase domain. Asterisks denote amino acids affected by point mutations in *sad-1* as well as the *ky289* stop codon, and ^ symbols denote truncation points in the *sad-1* (*ky344* and *ky326*) alleles.

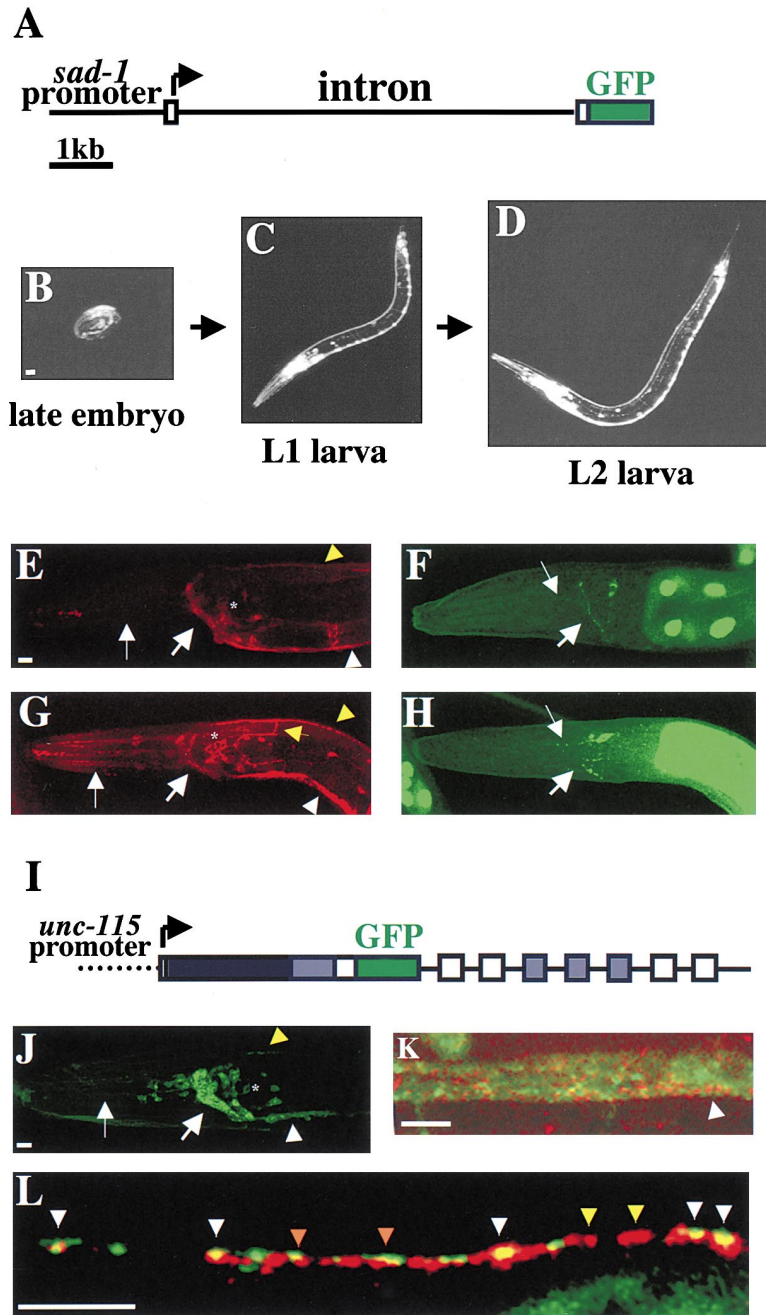


Figure 5. SAD-1 Expression and Protein Localization

(A–D) *sad-1* regulatory sequences were used to drive the expression of GFP (A). GFP was fused in frame to the second exon of *sad-1*. p_{sad-1} :GFP expression was seen exclusively in the nervous system beginning in the late embryo (B) and continuing through the life of the animal (C, D). (E, G) Anti-SAD-1 antibody staining of animals overexpressing SAD-1 from the endogenous promoter. (F, H) p_{snb-3} :SAD-1::GFP expression in the same animals. (E) In some animals, fluorescence was confined to axons of the nerve ring (thick arrow) and ventral (white arrowhead) and dorsal (yellow arrowhead) cords and to cell bodies (asterisk). No staining was observed in the sensory dendrites (thin arrow) or axon commissures. In these animals, ASI neuron morphology was normal (F). (G) In other animals, fluorescence was present in the dendrites (thin arrow) and commissures (yellow arrow) in addition to the axon and cell body staining seen in (E). (H) In these animals, axons were terminated (thick arrow) or otherwise defective, and some vesicle clusters appeared in the dendrite (thin arrow). (I) A full-length SAD-1::GFP fusion protein was expressed in the nervous system using the *unc-115* promoter. GFP was inserted in frame at amino acid 566 of the SAD-1 protein. Sequences 5' to GFP were from the *sad-1* cDNA, and sequences 3' were from the *sad-1* genomic clone. Shading of domain structure as in Figure 4(B), GFP in green. (J) SAD-1::GFP localized to puncta within the axons of the nerve ring (thick arrow) and ventral (white arrowhead) and dorsal (yellow arrowhead) nerve cords but was faint or absent in the dendrites (thin arrow) and synapse-poor commissures. Additionally, SAD-1::GFP was observed in cell bodies, where it was excluded from the nucleus (asterisk). These animals were fixed with formaldehyde to eliminate gut autofluorescence. (K) A higher magnification of the ventral cord in animals expressing $p_{unc-115}$:SAD-1::GFP (green) and costained with anti-SYD-2 (red) antibodies. Little colocalization of SAD-1::GFP and SYD-2 was evident (e.g., arrowhead). (L) A higher magnification of the dorsal cord in animals overexpressing SAD-1 from its own promoter and costained with anti-SAD-1 (red) and anti-SNT-1 (green) antibodies. Many SAD-1 and SNT-1 puncta overlapped (yellow color/white arrowheads) or were adjacent (red arrowheads). Most SNT-1 puncta were associated with SAD-1, but some SAD-1 puncta were not associated with SNT-1 (yellow arrowheads).

suggests that at more physiological levels SAD-1 preferentially localizes to synaptic regions.

In animals expressing $p_{unc-115}$:SAD-1::GFP, and in animals stained with anti-SAD-1 antibodies, fluorescence appeared as a combination of punctate and diffuse staining within the axon (Figures 5K and 5L). Costaining of animals expressing $p_{unc-115}$:SAD-1::GFP with anti-SYD-2 antibodies revealed that SAD-1 and SYD-2 are not extensively colocalized in the axons (Figure 5K). Costaining with anti-SAD-1 and anti-synaptotagmin antibodies revealed a partial colocalization of SAD-1 with

synaptic vesicles (Figure 5L). The SAD-1::GFP puncta were unaltered in *unc-104* mutants, indicating that SAD-1 does not depend on synaptic vesicles for localization (data not shown). Thus, it appears that SAD-1 is present in regions of the axon near synapses.

SAD-1 Can Function Cell-Autonomously in the VD and DD Motor Neurons to Promote Vesicle Clustering

The exclusive expression of SAD-1 in the nervous system suggests that SAD-1 functions cell-autonomously

in neurons to control presynaptic vesicle clustering. To test this hypothesis, we expressed SAD-1 protein in VD/DD motor neurons using the *unc-30* promoter and scored for the rescue of VD/DD SNB-1::GFP defects in *sad-1(ju53)* animals. 5/8 transgenic *unc-30::sad-1* lines exhibited rescue in which the SNB-1::GFP vesicle clusters in VD/DD neurons appeared more punctate and showed increased intensity compared to *sad-1(ju53)* animals. These results were comparable to the rescue of *sad-1(ju53)* animals by the cosmid F15A2 (3/7 lines rescued) or the *sad-1*-containing F15A2.dSacII genomic clone (4/10 lines rescued). The rescue of the VD/DD vesicle clustering defects of *sad-1* animals indicates that SAD-1 can function presynaptically to promote presynaptic differentiation.

SAD-1 Overexpression Causes Vesicle Protein Mislocalization to the Dendrite

Analysis of *sad-1* loss-of-function mutants suggested that SAD-1 is necessary for normal clustering of presynaptic vesicles. To further explore SAD-1 function we analyzed the effects of increased SAD-1 activity. SAD-1 activity was increased by generating transgenic animals with high levels of a wild-type SAD-1 transgene expressed under its own promoter. Overexpression of SAD-1 caused severe locomotion defects (Figures 6A and 6B) as well as axon guidance defects (see below). However, the pattern of SNB-1::GFP clusters in the axons was superficially normal when axons were not defective (Figure 6D). If anything, SAD-1 overexpressing animals appeared to have very bright clusters, suggesting an increased number of vesicles per cluster and possibly an increased number of SNB-1::GFP clusters in axons (Figures 6C to 6E). Surprisingly, ectopic SNB-1::GFP also appeared in the dendrite (Figures 6E to 6G). The dendritic fluorescence was punctate, resembling normal SNB-1::GFP axonal clusters in size and spacing. The increased amount of dendritic SNB-1::GFP is not a secondary consequence of axon outgrowth defects, as SNB-1::GFP mislocalization was not observed in other mutants that affected axon outgrowth [e.g., *unc-33(e204)* (Figure 6H) and data not shown]. These results show that increased SAD-1 activity can mislocalize SNB-1::GFP to ectopic locations.

To ask whether endogenous synaptic vesicle proteins were regulated similarly, SAD-1-overexpressing lines were stained with antibodies to synaptotagmin. This experiment revealed mislocalization of the endogenous synaptotagmin protein to dendritic regions in SAD-1-overexpressing lines (Figures 6I and 6J).

SAD-1 Regulates Axonal Branching and Termination

In *sad-1* animals the ASI neurons occasionally exhibited extra axon branches emanating from the primary axon in the area of the nerve ring (Figure 2G). To characterize this phenomenon more carefully at the single cell level, we examined the axonal morphology of another chemosensory neuron, the AWC neuron, in *sad-1* animals. p_{str-2} -GFP is expressed in a single AWC neuron (Troemel et al., 1999). AWC has an unbranched axon that extends ventrally and then anteriorly to the nerve ring, circles the nerve ring, and terminates on the contralateral ventral side of the animal (Figure 7A). In wild-type animals

expressing the p_{str-2} -GFP reporter the AWC axon invariably terminated at the ventral side. In 18% (n = 216) of *sad-1* animals the AWC axon failed to terminate at its correct position. Instead of terminating at the ventral side of the animal the AWC axon either reentered the nerve ring and returned to the dorsal side (Figure 7B) or traveled further posteriorly (Figure 7C) or anteriorly (Figure 7D). In addition, in 8% of these animals small ectopic branches emanated from the primary axon shaft (data not shown). In contrast to the ectopic sensory axon branches seen in mutants with altered electrical activity (Peckol et al., 1999), the branches in *sad-1* mutants were visible in early larvae and did not increase in penetrance over time. The failure of axons to terminate properly is not a secondary consequence of aberrant vesicle clustering; in *unc-104* mutants vesicle clusters are absent, yet axons terminate at the correct position and do not branch (Figure 7E). Conversely, the vesicle clustering defects cannot solely be a consequence of the axon defects, as they were more highly penetrant than the axon defects (>95% versus 26%).

Animals overexpressing SAD-1 exhibited a spectrum of axon defects in both the ASI and AWC sensory neurons: these included premature termination (Figures 7F, 7G, and 7J), axonal spreading and branching (Figure 7H), and severe guidance defects (Figures 6G and 7I). Occasionally, dendrite termination and branching were observed in the AWC neuron (Figure 7J). In the most severely affected strains with SAD-1 overexpression, ASI axon defects were present in 100% of the animals. In strains less severely affected for locomotion the most common defect of ASI and AWC axons was premature termination, suggesting that premature termination represents the less severe manifestation of SAD-1 overexpression. We presume that only very high levels of SAD-1 overexpression cause axon branching and misguidance and dendritic termination. We observed a close correlation between ASI neuron morphology defects and increased delocalization of SAD-1 protein in single animals. When SAD-1 was localized to synapse-rich regions, the ASI neurons appeared morphologically normal (Figures 5E and 5F). When overexpressed SAD-1 protein appeared at high levels in sensory dendrites and axonal commissures, ectopic vesicle proteins appeared in the dendrite and axons were malformed (Figures 5G and 5H).

Discussion

The SAD-1 Kinase Regulates Presynaptic Vesicle Clustering

A defining feature of presynaptic differentiation is the clustering of neurotransmitter-filled vesicles in precise apposition to postsynaptic neurotransmitter receptor clusters, facilitating the efficient transfer of information across the synapse. We have identified a novel serine/threonine kinase, SAD-1, that affects the size, shape, and position of vesicle clusters. Although we set out to identify molecules specifically required for synapses between neurons, *sad-1* mutants have defects both at neuron-to-neuron and at neuromuscular synapses. In *sad-1* mutant animals vesicle clusters are more diffusely distributed, mislocalized, and irregularly spaced in the ASI sensory axons. In VD and DD motor neurons, the

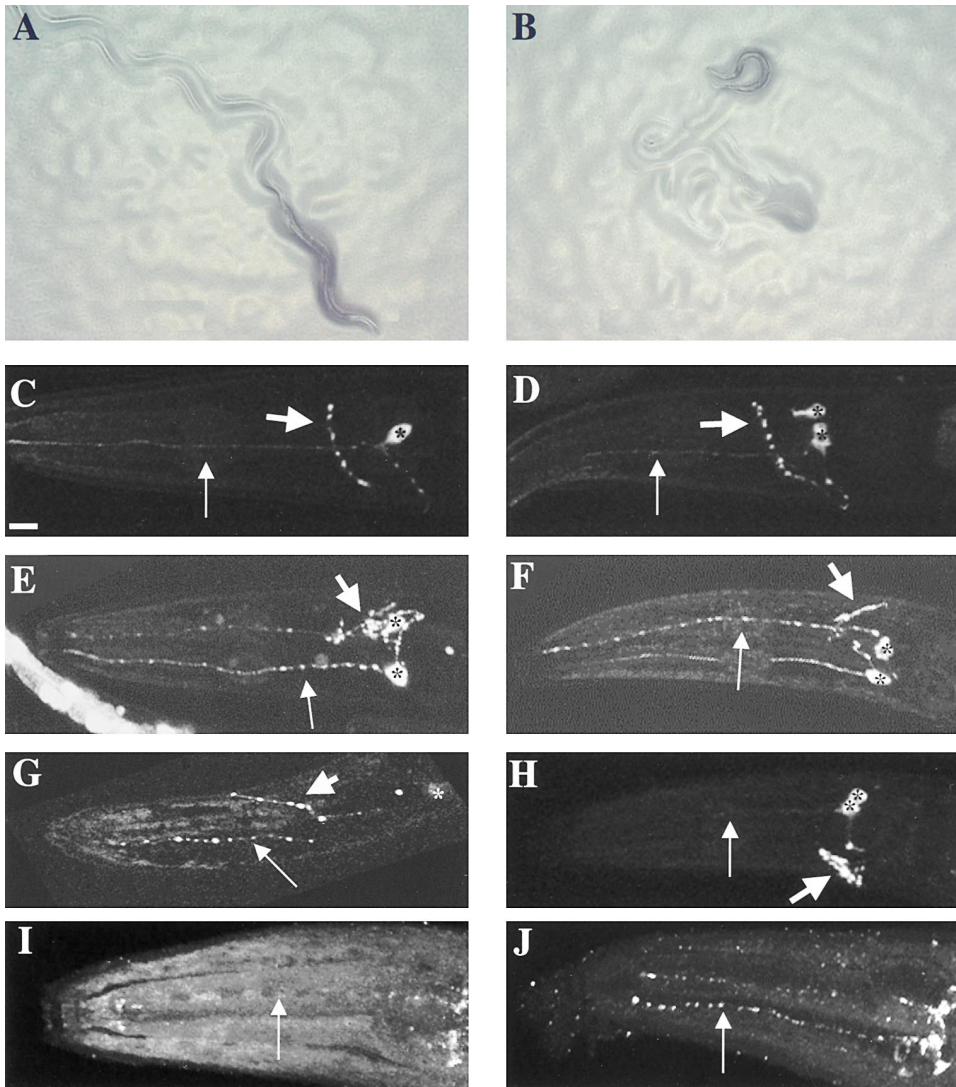


Figure 6. SAD-1 Overexpression Mislocalizes Synaptic Vesicle Proteins to Dendrites

(A) Wild-type animals moved in a sinusoidal pattern on a bacterial lawn. (B) Animals overexpressing SAD-1 from the endogenous promoter moved very little from where they were placed on the lawn, and their locomotion was severely uncoordinated. (C–H) Confocal epifluorescence micrographs showing expression of SNB-1::GFP in the ASI neurons of wild-type (C), SAD-1 overexpressing (D–G), and *unc-33(e204)* (H) animals. Anterior is left and dorsal is up. Thin arrows point to dendrites, thick arrows point to axons, and asterisks denote cell bodies. SNB-1::GFP clusters in the axons of SAD-1 overexpressing animals appeared more numerous (D, E) and perhaps more sharply defined (D) than the SNB-1::GFP clusters in the axons of wild-type animals (C). In some SAD-1 overexpressing animals, SNB-1::GFP was present in the dendrites (E–G). Compare this to the faint, diffuse SNB-1::GFP fluorescence occasionally seen in the dendrites of wild-type animals (C). The axons of SAD-1 overexpressing animals were often prematurely terminated or misguided (E–G). In *unc-33(e204)* animals axons were affected to a similar degree, but SNB-1::GFP was not mislocalized to the dendrite (H). (I, J) Wild-type animals and animals overexpressing SAD-1 were stained with antibodies against synaptotagmin, an endogenous synaptic vesicle protein. The dendritic regions of amphid neurons (arrow) in wild-type animals showed no staining (I), whereas bright synaptotagmin puncta (arrow) were observed in SAD-1 overexpressing animals (J).

vesicles are diffuse, a result that was confirmed by electron micrographs that showed a defect in vesicle clustering.

SAD-1 does not appear to control all aspects of pre-synaptic differentiation. The normal localization of the active zone protein SYD-2 and electron micrographs of synapses show that SAD-1 is not necessary for active zone formation in motor neurons. In *syd-2* mutants, both vesicle clusters and active zones are wider than normal (Zhen and Jin, 1999). The different phenotypes of *syd-2*

and *sad-1* and the additive defects in *syd-2; sad-1* double mutants suggest that SYD-2 and SAD-1 function in separate aspects of synapse formation. Another gene involved in synapse formation, *rpm-1*, shows a distinct VD/DD synaptic defect with multiple active zones per vesicle cluster (Zhen et al., 2000). Both *rpm-1(sad-3)* and *sad-1* mutations were identified in the ASI synaptic screens and the VD/DD synaptic screens. At the level of SNB-1::GFP expression, *sad-1* mutants have a severe defect in ASI and a more subtle defect in VD/DD,

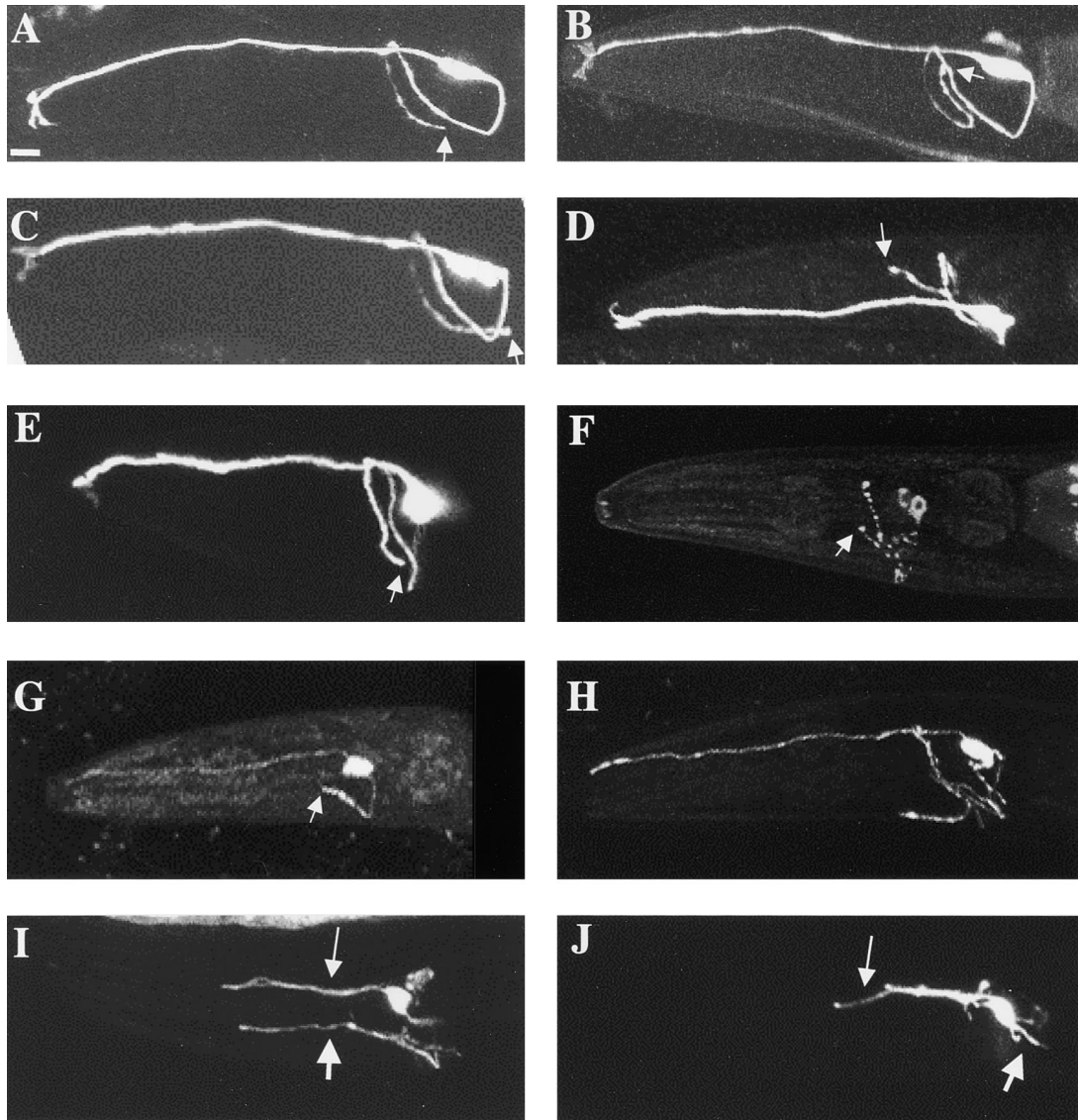


Figure 7. Reciprocal Axon Phenotypes in *sad-1* Mutants and SAD-1 Overexpressing Animals

Confocal epifluorescence micrographs of wild-type (A), *sad-1(ky332)* (B–D), *unc-104(e1265)* (E), and SAD-1 overexpressing (F–J) animals expressing p_{str-2} :GFP (A–E, G–J) or p_{str-3} :SNB-1::GFP (F). Anterior is left and dorsal is up. p_{str-2} :GFP labels a single AWC neuron. In (A–G) arrows denote the axon termination points. In wild-type animals, the axon of the AWC neuron terminates at the ventral side of the animal (A). In 18% of *sad-1(ky332)* mutants, the AWC axon fails to terminate at the proper position and either reenters the nerve ring (B) or continues posteriorly (C) or anteriorly (D). In *unc-104(e1265)* animals, the AWC axon terminates at the proper location 100% of the time (E). In SAD-1 overexpressing animals, the ASI (F) and AWC (G) axons were often prematurely terminated. In other SAD-1 overexpressing animals, the axons were branched (H) and misguided (thick arrow) (I). Occasionally, dendrites of AWC neurons were also prematurely terminated (thin arrow) (I), and in rare cases the axon was missing (thick arrow) and the dendrite was prematurely terminated and misshapen (thin arrow) (J).

whereas *rpm-1* mutants have a severe defect in VD/DD and a more subtle defect in ASI (Zhen et al., 2000, this work, and data not shown). Thus SAD-1 acts in concert with other regulatory molecules to coordinate different facets of presynaptic development and may have a more or less important role in different classes of neurons.

Overexpression of SAD-1 induces the appearance of SNB-1::GFP in sensory dendrites, in structures that resemble vesicle clusters in size, shape, and spacing. We do not know to what extent these ectopic structures express other synaptic vesicle proteins and participate in neurotransmitter release, nor do we have evidence

for the presence of ectopic active zones in the dendrite. SAD-1 is normally localized to axons, but overexpression of SAD-1 causes some SAD-1 to be mislocalized to the dendrite, where it could recruit synaptic vesicle proteins.

Some SAD-1 protein colocalizes with the synaptic vesicle protein synaptotagmin, but SAD-1 is not dependent on synaptic vesicles for its localization to axons. In addition, SAD-1 does not colocalize with the active zone protein SYD-2. These results suggest that SAD-1 is present at or near synapses, perhaps in perisynaptic regions, but since they are based on overexpressed

SAD-1, the normal localization pattern might be more discrete. One model is that the interaction between pre- and postsynaptic cells establishes active zones through pathways that are independent of SAD-1 function; subsequently, SAD-1 becomes locally activated near active zones and recruits and shapes vesicle clusters. It might do so directly or indirectly by regulating trafficking of vesicles along microtubules. In *sad-1* mutants vesicle clusters are diffuse and disorganized in relation to active zones; however, SAD-1 is not absolutely required for vesicle clustering as looser vesicle clusters form in null *sad-1* animals. Upon overexpression, SAD-1 activity may become active zone-independent and stimulate accumulation of synaptic vesicle proteins in ectopic locations. Several mutations in *sad-1* map to the kinase domain, indicating that the kinase activity of SAD-1 is critical for its function. We propose that the phosphorylation of downstream targets by SAD-1 promotes the clustering of synaptic vesicles and mediates an interaction between vesicle clusters and active zones.

Highly conserved SAD-1 homologs are found in invertebrates and vertebrates, suggesting that SAD-1 has a conserved function in all animals. Homology in the kinase domain of SAD-1 places it in the AMPK family of serine/threonine kinases (Carling et al., 1994). Within the *C. elegans* AMPK family SAD-1 shares highest similarity with PAR-1. PAR-1 is required for asymmetric cell divisions along the anterior-posterior (A-P) axis and localizes to the posterior cortex of the one-cell embryo (Guo and Kemphues, 1995). *par-1* has a central role in embryonic polarity: in *par-1* mutants P-granules and cell fate determinants such as SKN-1 fail to segregate asymmetrically in A-P cell divisions, and there are defects in mitotic spindle rotation. A PAR-1 ortholog in *Drosophila* also plays a central role in embryonic polarity (Shulman et al., 2000), and mammalian PAR-1 homologs are implicated in epithelial polarity (Bohm et al., 1997). There are three vertebrate PAR-1-related kinases: MARK1, MARK2/EMK1, and MARK3/C-TAK1/Kp78. MARK1 and MARK2 (MAP/microtubule affinity-regulating kinases 1 and 2) were identified biochemically in the rat based on their ability to phosphorylate *tau*, an axonal MAP (microtubule-associated protein) and decrease its affinity for microtubules (Drewes et al., 1995). Overexpression of MARK1 or MARK2 in fibroblasts disrupts microtubules and causes a loss of polarity (Drewes et al., 1997). MARK3, which phosphorylates Cdc25C phosphatase (Peng et al., 1998), localizes to the apical domain of epithelial cells (Parsa, 1988). Thus the PAR-1-related proteins share a polarized location and possibly the ability to regulate the cytoskeleton and cell polarity. Intriguingly, the ascidian SAD-1 homolog was identified in a search for mRNAs that localize to the posterior pole of the one-cell embryo (Sasakura et al., 1998). This localization suggests that PAR-1 and SAD-1 may have related functions in cell polarity, though we have no evidence that *sad-1* is expressed in early embryos.

The SAD-1 Kinase May Regulate the Transition from Axon Outgrowth to Synapse Formation

During neuronal development, the end of axon outgrowth is coupled to the initiation of synaptic differentiation. In mouse mutants in which synaptic differentiation

is blocked, such as the agrin and MuSK knockouts, axons extend past their targets (Gautam et al., 1996; DeChiara et al., 1996). Similarly, in *sad-1* mutants axons often fail to terminate appropriately and sometimes form extra branches. Conversely, overexpression of SAD-1 causes axons to terminate prematurely. The reciprocal phenotypes of *sad-1* loss of function and SAD-1 overexpression suggest that SAD-1 has an instructive role in regulating axon outgrowth. We propose that SAD-1 has two functions: the first is to promote vesicle clustering and the second is to signal axons to stop elongating. We speculate that SAD-1 may couple the end of axon outgrowth with the beginning of presynaptic differentiation, perhaps by responding to retrograde signals from the postsynaptic target.

It is unlikely that the axon defects we see are secondary to the vesicle clustering defects. First, in *unc-104* animals, which lack vesicle clusters, axons never grow past their target. Second, in *unc-13* animals, in which vesicle clusters are larger and better defined than normal, axons never terminate prematurely (Kang Shen and C. I. B., unpublished observations). These observations argue that the functions of SAD-1 in vesicle clustering do not cause axon termination.

The *rpm-1* mutant that disrupts synaptic differentiation destabilizes an axon branch in the PLM mechanosensory neurons (Schaefer et al., 2000). This effect is opposite the effect that we observe in ASI in *sad-1* mutants, but emphasizes the general link between axon branching and synapse formation.

In the axonal growth cone actin polymerization and microtubule structure are dynamically controlled, thereby promoting directed motility toward a target (reviewed in Suter and Forscher, 1998). The transition from a highly motile state to one of strong, stable adhesion at the synapse likely involves modification of the cytoskeleton (Grady et al., 2000). One possibility is that SAD-1 regulates the microtubule cytoskeleton, like the related PAR-1 and the MARK kinases.

SAD-1 and PAR-1 May Define a Novel Family of Kinases More Generally Involved in Controlling Cell Polarity

Some molecules implicated in synapse formation, like cadherins, are symmetrically expressed in the pre- and postsynaptic cell, yet the two cells accumulate different proteins at the synapse because of their intrinsic neuronal polarity: vesicle clusters and release machinery are localized to the presynaptic axon and neurotransmitter receptors to the dendrite. SAD-1's similarity to the cell polarity kinase PAR-1 suggests that it might play a role in defining polarity in neurons. SAD-1 localizes asymmetrically in neurons to synaptic regions within the axon. SAD-1 does not seem to be essential for neuronal polarity, because in *sad-1* mutants the ASI sensory axon, though disorganized, is still different from the dendrite. However, *sad-1* loss-of-function mutants exhibit defects in polarity of the DD motor neurons, with vesicle mislocalization to inappropriate processes. In addition, when SAD-1 is overexpressed and appears in dendrites, the ASI sensory dendrites accumulate axonal vesicle proteins. Interestingly, Wnt signals, which promote mossy fiber presynaptic differentiation, can also regulate cell

polarity (Schlesinger et al., 1999; Hall et al., 2000). SAD-1 may help link intrinsic axon-dendrite polarity to external signals that promote presynaptic development.

Experimental Procedures

Strains and Maintenance

Wild-type animals were *C. elegans* variety Bristol, strain N2. Animals were grown at 20°C on HB101 bacteria and maintained according to standard methods (Brenner, 1974). Some strains were provided by the *Caenorhabditis* Genetic Center, which is supported by the National Institutes of Health.

Screen for SNB-1::GFP Defects in ASI, VD, and DD Neurons

$p_{\text{SNB-1}}::\text{SNB-1}::\text{GFP}$ was constructed by cloning a SphI-NheI PCR product containing 3kb of *str-3* upstream sequences into pSB121.51 (Nonet, 1999); an enhanced GFP from pPD95.75 was swapped with the GFP of pSB121.51 as an AgeI-ApaI fragment to increase fluorescence intensity. *lin-15(n765ts)* mutant animals were injected with $p_{\text{SNB-1}}::\text{SNB-1}::\text{GFP}$ at 100 ng/ μl and a *lin-15(+)* pJM23 plasmid as a coinjection marker at 50 ng/ μl (Huang et al., 1994). Transformants were maintained by picking animals rescued for the *lin-15* multivulval phenotype. The transgenic array was integrated into the genome using psoralen mutagenesis. One integrant, CX3572 *kyls105; lin-15(n765ts)*, was outcrossed four times and used for subsequent analysis. *kyls105; lin-15(n765ts)* animals were mutagenized with EMS. Approximately 100,000 F2 progeny were enriched for a lack of chemotaxis to a 1:200 point source of benzaldehyde and from this enrichment ~10,000 were screened visually for SNB-1::GFP defects. A screen for SNB-1::GFP defects in VD/DD neurons has been previously described (Zhen and Jin, 1999; Zhen et al., 2000).

Light Microscopy

Vesicle clusters of ASI neurons were visualized in *kyls105; lin-15(n765ts)* animals, and vesicle clusters of VD and DD motor neurons were visualized with an integrated *unc-25-SNB-1::GFP* transgene (CZ333, *juls1 X*) (Hallam and Jin, 1998). AWC axons were visualized with an integrated $p_{\text{SNB-1}}::\text{SNB-1}::\text{GFP}$ transgene [strain CX3621 *kyls136 lin-15(n765ts X)*] (Troemel et al., 1999). Living animals were mounted on 2% agarose pads containing 3 mM sodium azide. Fluorescence was visualized using a Nikon Eclipse TE300 equipped with a Biorad MRC-1024 Laser Scanning Confocal Imaging System. Images were captured at 60 \times magnification and processed using the NIH Image and Adobe Photoshop programs.

Electron Microscopic Analysis of *sad-1(ky289)* Animals

sad-1(ky289) animals without any SNB-1::GFP markers were used for EM analysis. Two young adult *sad-1(ky289)* animals were fixed in glutaraldehyde as previously described (Jin et al., 1999). Regions between the posterior pharyngeal bulb and the vulva were sectioned. Two hundred sections of 50–60 nm thickness were collected for each sample and the ventral nerve cords were photographed. VD GABAergic NMJs were identified based on the position and shape of the varicosities that were filled with synaptic vesicles and the appearance of darkly stained active zones directly opposing the muscle arms. N2 animals were used as wild-type controls.

The distribution of vesicles was analyzed by examining serial sections through ten presynaptic termini and counting the number of vesicles in each section. Because the size of presynaptic termini and the number of synaptic vesicles differ at individual neuromuscular junctions, we normalized each synapse by comparing the number of vesicles in each section to the number of vesicles at the active zone region. This ratio is plotted in Figure 3. For six *sad-1* synapses, the vesicles at two adjacent synapses overlapped. This made it impossible to estimate the vesicle distribution on that side of the active zone (the half-synapse). The six half-synapses with overlap were excluded from the analysis in Figure 3; as a result, this figure underestimates the total extent of vesicle diffusion in *sad-1* mutants. Because of the overlap between synapses, we could not count the total number of vesicles per synapse accurately in all cases. For the wild-type synapses examined here, we observed 178 ± 23 vesicles per synapse; for *sad-1(ky289)* synapses vesicle numbers ranged from 170 to 500.

sad-1 Mapping

sad-1(ky332) was mapped with respect to Tc1 transposable element polymorphisms in the DP13 strain (Williams, 1995) by following the SNB-1::GFP defects. *sad-1* was localized to LGX between the stP72 and stP2 polymorphisms. Three-factor mapping was conducted to further localize *sad-1(ky332)* on LGX. 4/19 *unc-9(e101)* non-*unc-3(e95)* recombinants were mutant for *sad-1*. A restriction fragment polymorphism associated with *odr-1(1933)* was used to map *sad-1(ky332)* further. *unc-9(e101) sad-1(ky332) +/+ + odr-1(1933)* animals segregated 14/14 *unc-9* non-*sad-1* animals that contained the *odr-1(1933)* polymorphism. These mapping data placed *sad-1* right of *unc-9* and very close to *odr-1* on LGX.

Germline Transformation Rescue

Transgenic strains were created as previously described (Mello and Fire, 1995). Multiple lines from each injection were characterized for rescue of the SNB-1::GFP phenotype. Cosmids spanning the region between *unc-9* and *odr-1* were injected at 20 ng/ μl in pools of five to seven cosmids using the pJM67 $p_{\text{ent-2}}$ GFP plasmid at 12 ng/ μl as a coinjection marker (Fukushige et al., 1998). Transformants were maintained by picking animals expressing *elt-2::GFP* in the intestine. Cosmids from the rescuing pool were injected individually or in pairs at 100 ng/ μl , identifying F15A2 as the single rescuing cosmid. A version of F15A2 deleted for a SacII fragment and a subclone containing a 13.8 kb SacII-AvrII fragment of F15A2 rescued the *sad-1* mutant phenotype at 50 to 100 ng/ μl . The subclone contained 0.3 kb upstream of the start codon, the entire *sad-1* open reading frame, the *sad-1* 3'UTR, and 0.25 kb of downstream sequence.

cDNA Isolation and Allele Sequencing

A partial cDNA yk410d1 corresponding to the predicted ORF F15A2.6 was obtained from Yuji Kohara. The 5' end of the *sad-1* coding region was identified by RT-PCR from wild-type N2 RNA prepared by Trizol extraction (gift of E. Troemel). First-strand cDNAs were reverse transcribed by the primer F15cD-3A 5'-cgctattcttcccc gaataac-3'. This cDNA served as a template for PCR amplification with the SL1 and F15cD-3A primers for 30 cycles at 94°C for 30 s, 52°C for 1 min, 72°C for 1 min on an MJ Research thermal cycler. A second, hemi-nested amplification was carried out under identical conditions using 1 μl of the original reaction with the SL1 and F15cD-3B 5'-cgaataactctggacatgcataatgtggagatcc-3' primers. A 0.75 kb band was isolated and subcloned into the BamHI-BsmBI sites of yk410d1 to create a full-length *sad-1* cDNA. The *sad-1* cDNA was sequenced, and the genomic organization of *sad-1* was determined by aligning the cDNA with the reported genomic sequence from the *C. elegans* Sequencing Consortium (1998). To identify the mutations in *sad-1* alleles, the open reading frame and splice junctions of the mutant alleles were PCR amplified from two separate genomic DNA preparations of the mutant strains. PCR fragments were pooled and sequenced on both strands using an ABI sequencing machine (UCSF HHMI DNA facility).

Overexpression and Motor Neuron-Specific Rescue Experiments

For overexpression studies, the SacII deletion version of F15A2 was injected at 240 ng/ μl with $p_{\text{ent-2}}$ GFP at 12 ng/ μl into *kyls105; lin-15(n765ts)* animals and integrated into the genome using psoralen mutagenesis. The integrant *kyls214 kyls105; lin-15(n765ts)* was used for further analysis.

To specifically express SAD-1 in VD and DD neurons, a mini-gene construct, c4EA, was first derived from the *sad-1* cDNA clone by replacing the EcoRI-SacII cDNA fragment with a 3.9 kb genomic piece from F15A2. A 5.7 kb BamHI-ApaI fragment from c4EA that contains *sad-1* mini-gene plus 3' untranslated region was cloned in the BamHI/ApaI sites of pSC316 (M. Z. and Y. J., unpublished observation) that contains the *unc-30* promoter to generate pCZ335. *sad-1(ju53)* animals were injected with pCZ335, F15A2, and F15A2.dSacII and scored for SNB-1::GFP phenotypes in VD and DD neurons.

sad-1 Expression Analysis

A reporter $p_{\text{sad-1}}::\text{GFP}$ fusion was constructed by cloning a PstI-BamHI PCR product corresponding to nucleotides 34884–26254 of F15A2 in frame into the GFP expression vector pPD95.75 (a gift from A.

Fire, S. Xu, J. Ahnn, and G. Seydoux). A translational $p_{unc-115}$ -SAD-1::GFP fusion was made by inserting a PCR product, corresponding to 1.6kb of upstream *unc-115* sequences, as a NotI-BamHI fragment into the c4EA mini-gene. Into this subclone GFP from pPD102.33 (a gift from A. Fire, S. Xu, J. Ahnn, and G. Seydoux) was inserted in frame at an EcoRI site corresponding to amino acid 566 of the SAD-1 protein. The *unc-115* promoter was used because it expressed SAD-1::GFP at lower levels than the endogenous *sad-1* promoter and consequently gave less frequent overexpression phenotypes. The p_{sad-1} -GFP and $p_{unc-115}$ -SAD-1::GFP transgenes were injected at 100 and 30 ng/ μ l into *lin-15(n765ts)* animals using the *lin-15(+)* pJM23 plasmid at 30 ng/ μ l as a coinjection marker (Huang et al., 1994). The *sad-1* expression and localization patterns were assessed in variably mosaic animals that contained the transgenes as unstable extrachromosomal DNA. In *C. elegans* the first intron is often very large and is thought to contribute regulatory information; anecdotally, we note that 3.6 kb of 3' first intron sequences was able to drive expression of GFP in a subset of neurons (data not shown).

Generation of SAD-1 Antibodies

A 6His-GST-SAD-1 fusion protein containing amino acids 422–559 (from a BgIII-Sall cDNA fragment) was expressed in bacteria using the pQE41 vector (Qiagen), purified following the manufacturer's protocol, and used to immunize rats (Covance). Crude polyclonal antisera was precleared against fixed *sad-1(ky289)* animals [methanol (5') and acetone (5'), dry ice frozen and pulverized] and used at 1:20 dilution on whole mounts. Anti-GFP, anti-SYD-2 (Zhen and Jin, 1999), and anti-SNT-1 antibodies (Nonet et al., 1993) were used as described. Cy5-conjugated goat anti-rat (Zymed) and Cy3-conjugated goat anti-rabbit (Jackson ImmunoResearch) IgG secondary antibodies were used at 1:25 and 1:300 dilutions. Secondary antibodies were similarly precleared against fixed wild-type animals. Whole-mount immunofluorescence staining was performed as described in Finney and Ruvkun (1990).

Protein Sequence Analysis

Phylogenetic analysis was performed using the ClustalW (Thompson et al., 1994) and NJplot programs. Sequences used corresponded to amino acids 47–297 of the SAD-1 kinase domain. Protein alignment was performed in MacVector. The Genbank identifier numbers for the sequences used in the alignment and/or tree are as follows: *Drosophila melanogaster* CG6114, gij7294217, and CG8201 (*Drosophila* PAR-1), gij7302464; *Halocynthia roretzi* HrPOPK-1, gij3172111; *Caenorhabditis elegans* PAR-1, gij733122, and *unc-43* CaM Kinase II, gij1118007; *Rattus norvegicus* MARK1, gij2052188, and MARK2, gij2052190; *Homo sapiens* CAA07196 EST, gij3217028, MARK3, gij4505102, and AMP Kinase α 1, gij5453964; *Saccharomyces cerevisiae* *Sfn1p*, gij6320685.

Acknowledgments

We thank Shai Shaham and Josh Sanes for comments on the manuscript, Kang Shen and Noelle L'Etoile for discussions and ideas, Bob Herman and the *Caenorhabditis* Genetic Center for strains, Mike Nonet for the SNB-1::GFP clone and anti-SNT-1 antibodies, Yuji Kohara for cDNAs, Andy Fire for GFP vectors, Jim McGhee for *elt-2::GFP*, and Shannon Grantner and Hai Nguyen for technical support. J. G. C. was supported by a Howard Hughes Medical Institute Predoctoral Fellowship and a UCSF Chancellor's Fellowship, and C. I. B. is an Investigator of the Howard Hughes Medical Institute. M. Z. was supported by a Human Frontier Science Program Long Term Postdoctoral Fellowship. This work was supported by the Howard Hughes Medical Institute and a US PHS research grant to Y. J.

Received May 25, 2000; revised October 17, 2000.

References

Adams, M.D., et al. (2000). The genome sequence of *Drosophila melanogaster*. *Science* 287, 2185–2195.
Avery, L., Bargmann, C.I., and Horvitz, H.R. (1993). The *Caenorhabditis elegans* *unc-31* gene affects multiple nervous system-controlled functions. *Genetics* 134, 455–464.

Bargmann, C.I., and Horvitz, H.R. (1991). Control of larval development by chemosensory neurons in *Caenorhabditis elegans*. *Science* 251, 1243–1246.
Bohm, H., Brinkmann, V., Drab, M., Henske, A., and Kurzchalia, T.V. (1997). Mammalian homologues of *C. elegans* PAR-1 are asymmetrically localized in epithelial cells and may influence their polarity. *Curr. Biol.* 7, 603–606.
Brenner, S. (1974). The genetics of *Caenorhabditis elegans*. *Genetics* 77, 71–94.
Butz, S., Okamoto, M., and Sudhof, T.C. (1998). A tripartite protein complex with the potential to couple synaptic vesicle exocytosis to cell adhesion in brain. *Cell* 94, 773–782.
Carling, D., Aguan, K., Woods, A., Verhoeven, A.J., Beri, R.K., Brennan, C.H., Sidebottom, C., Davison, M.D., and Scott, J. (1994). Mammalian AMP-activated protein kinase is homologous to yeast and plant protein kinases involved in the regulation of carbon metabolism. *J. Biol. Chem.* 269, 11442–11448.
C. elegans Sequencing Consortium (1998). Genome sequence of the nematode *C. elegans*: a platform for investigating biology. *Science* 282, 2012–2018.
DeChiara, T.M., Bowen, D.C., Valenzuela, D.M., Simmons, M.V., Poueymirou, W.T., Thomas, S., Kinetz, E., Compton, D.L., Rojas, E., Park, J.S., et al. (1996). The receptor tyrosine kinase MuSK is required for neuromuscular junction formation in vivo. *Cell* 85, 501–512.
Drewes, G., Trinczek, B., Illenberger, S., Biernat, J., Schmitt-Ulms, G., Meyer, H.E., Mandelkow, E.M., and Mandelkow, E. (1995). Microtubule-associated protein/microtubule affinity-regulating kinase (p110mark). A novel protein kinase that regulates tau-microtubule interactions and dynamic instability by phosphorylation at the Alzheimer-specific site serine 262. *J. Biol. Chem.* 270, 7679–7688.
Drewes, G., Ebneth, A., Preuss, U., Mandelkow, E.M., and Mandelkow, E. (1997). MARK, a novel family of protein kinases that phosphorylate microtubule-associated proteins and trigger microtubule disruption. *Cell* 89, 297–308.
Fenster, S.D., Chung, W.J., Zhai, R., Cases-Langhoff, C., Voss, B., Garner, A.M., Kaempf, U., Kindler, S., Gundelfinger, E.D., and Garner, C.C. (2000). Piccolo, a presynaptic zinc finger protein structurally related to bassoon. *Neuron* 25, 203–214.
Finney, M., and Ruvkun, G. (1990). The *unc-86* gene product couples cell lineage and cell identity in *C. elegans*. *Cell* 63, 895–905.
Fukushige, T., Hawkins, M.G., and McGhee, J.D. (1998). The GATA-factor *elt-2* is essential for formation of the *Caenorhabditis elegans* intestine. *Dev. Biol.* 198, 286–302.
Gautam, M., Noakes, P.G., Moscoso, L., Rupp, F., Scheller, R.H., Merlie, J.P., and Sanes, J.R. (1996). Defective neuromuscular synaptogenesis in agrin-deficient mutant mice. *Cell* 85, 525–535.
Glass, D.J., Bowen, D.C., Stitt, T.N., Radziejewski, C., Bruno, J., Ryan, T.E., Gies, D.R., Shah, S., Mattsson, K., Burden, S.J., et al. (1996). Agrin acts via a MuSK receptor complex. *Cell* 85, 513–523.
Grady, R.M., Zhou, H., Cunningham, J.M., Henry, M.D., Campbell, K.P., and Sanes, J.R. (2000). Maturation and maintenance of the neuromuscular synapse: genetic evidence for roles of the dystrophin–glycoprotein complex. *Neuron* 25, 279–293.
Guo, S., and Kemphues, K.J. (1995). *par-1*, a gene required for establishing polarity in *C. elegans* embryos, encodes a putative Ser/Thr kinase that is asymmetrically distributed. *Cell* 81, 611–620.
Hall, A.C., Lucas, F.R., and Salinas, P.C. (2000). Axonal remodeling and synaptic differentiation in the cerebellum is regulated by WNT-7a signaling. *Cell* 100, 525–535.
Hallam, S.J., and Jin, Y. (1998). *lin-14* regulates the timing of synaptic remodeling in *Caenorhabditis elegans*. *Nature* 395, 78–82.
Hosaka, M., Hammer, R.E., and Sudhof, T.C. (1999). A phospho-switch controls the dynamic association of synapsins with synaptic vesicles. *Neuron* 24, 377–387.
Huang, L.S., Tzou, P., and Sternberg, P.W. (1994). The *lin-15* locus encodes two negative regulators of *Caenorhabditis elegans* vulval development. *Mol. Biol. Cell.* 5, 395–411.
Jin, Y., Jorgensen, E., Hartwig, E., and Horvitz, H.R. (1999). The

- Caenorhabditis elegans* gene *unc-25* encodes glutamic acid decarboxylase and is required for synaptic transmission but not synaptic development. *J. Neurosci.* **19**, 539–548.
- Kohmura, N., Senzaki, K., Hamada, S., Kai, N., Yasuda, R., Watanabe, M., Ishii, H., Yasuda, M., Mishina, M., and Yagi, T. (1998). Diversity revealed by a novel family of cadherins expressed in neurons at a synaptic complex. *Neuron* **20**, 1137–1151.
- Lu, B., Greengard, P., and Poo, M.M. (1992). Exogenous synapsin I promotes functional maturation of developing neuromuscular synapses. *Neuron* **8**, 521–529.
- Lundquist, E.A., Herman, R.K., Shaw, J.E., and Bargmann, C.I. (1998). UNC-115, a conserved protein with predicted LIM and actin-binding domains, mediates axon guidance in *C. elegans*. *Neuron* **21**, 385–392.
- Matsuura, A., Tsukada, M., Wada, Y., and Ohsumi, Y. (1997). Apg1p, a novel protein kinase required for the autophagic process in *Saccharomyces cerevisiae*. *Gene* **192**, 245–250.
- Mello, C., and Fire, A. (1995). DNA transformation. *Methods Cell Biol.* **48**, 451–482.
- Noakes, P.G., Gautam, M., Mudd, J., Sanes, J.R., and Merlie, J.P. (1995). Aberrant differentiation of neuromuscular junctions in mice lacking s-laminin/laminin beta 2. *Nature* **374**, 258–262.
- Nonet, M.L. (1999). Visualization of synaptic specializations in live *C. elegans* with synaptic vesicle protein-GFP fusions. *J. Neurosci. Methods* **89**, 33–40.
- Nonet, M.L., Grundahl, K., Meyer, B.J., and Rand, J.B. (1993). Synaptic function is impaired but not eliminated in *C. elegans* mutants lacking synaptotagmin. *Cell* **73**, 1291–1305.
- Nonet, M.L., Holgado, A.M., Brewer, F., Serpe, C.J., Norbeck, B.A., Holleran, J., Wei, L., Hartwig, E., Jorgensen, E.M., and Alfonso, A. (1999). UNC-11, a *Caenorhabditis elegans* AP180 homologue, regulates the size and protein composition of synaptic vesicles. *Mol. Biol. Cell.* **10**, 2343–2360.
- Ogura, K., Wicky, C., Magnenat, L., Tobler, H., Mori, I., Muller, F., and Ohshima, Y. (1994). *Caenorhabditis elegans unc-51* gene required for axonal elongation encodes a novel serine/threonine kinase. *Genes Dev.* **8**, 2389–2400.
- Otsuka, A.J., Jeyaprakash, A., Garcia-Anoveros, J., Tang, L.Z., Fisk, G., Hartshorne, T., Franco, R., and Born, T. (1991). The *C. elegans unc-104* gene encodes a putative kinesin heavy chain-like protein. *Neuron* **6**, 113–122.
- Parsa, I. (1988). Loss of a Mr 78,000 marker in chemically induced transplantable carcinomas and primary carcinoma of human pancreas. *Cancer Res.* **48**, 2265–2272.
- Peckol, E.L., Zallen, J.A., Yarrow, J.C., and Bargmann, C.I. (1999). Sensory activity affects sensory axon development in *C. elegans*. *Development* **126**, 1891–1902.
- Peng, C.Y., Graves, P.R., Ogg, S., Thoma, R.S., Byrnes, M.J., 3rd, Wu, Z., Stephenson, M.T., and Piwnicka-Worms, H. (1998). C-TAK1 protein kinase phosphorylates human Cdc25C on serine 216 and promotes 14–3-3 protein binding. *Cell. Growth. Differ.* **9**, 197–208.
- Porter, B.E., Weis, J., and Sanes, J.R. (1995). A motoneuron-selective stop signal in the synaptic protein S-laminin. *Neuron* **14**, 549–559.
- Pulak, R., and Anderson, P. (1993). mRNA surveillance by the *Caenorhabditis elegans smg* genes. *Genes Dev.* **7**, 1885–1897.
- Ren, P., Lim, C.S., Johnsen, R., Albert, P.S., Pilgrim, D., and Riddle, D.L. (1996). Control of *C. elegans* larval development by neuronal expression of a TGF-beta homolog. *Science* **274**, 1389–1391.
- Rosahl, T.W., Spillane, D., Missler, M., Herz, J., Selig, D.K., Wolff, J.R., Hammer, R.E., Malenka, R.C., and Sudhof, T.C. (1995). Essential functions of synapsins I and II in synaptic vesicle regulation. *Nature* **375**, 488–493.
- Sanes, J.R., and Lichtman, J.W. (1999). Development of the vertebrate neuromuscular junction. *Annu. Rev. Neurosci.* **22**, 389–442.
- Sasakura, Y., Ogasawara, M., and Makabe, K.W. (1998). Maternally localized RNA encoding a serine/threonine protein kinase in the ascidian, *Halocynthia roretzi*. *Mech. Dev.* **76**, 161–163.
- Schackwitz, W.S., Inoue, T., and Thomas, J.H. (1996). Chemosensory neurons function in parallel to mediate a pheromone response in *C. elegans*. *Neuron* **17**, 719–728.
- Schaefer, A.M., Hadwiger, G.D., and Nonet, M.L. (2000). *rpm-1*, a conserved neuronal gene that regulates targeting and synaptogenesis in *C. elegans*. *Neuron* **26**, 345–356.
- Scheiffele, P., Fan, J., Choih, J., Fetter, R., and Serafini, T. (2000). Neuroligin expressed in nonneuronal cells triggers presynaptic development in contacting axons. *Cell* **101**, 657–669.
- Schlesinger, A., Shelton, C.A., Maloof, J.N., Meneghini, M., and Bowerman, B. (1999). Wnt pathway components orient a mitotic spindle in the early *Caenorhabditis elegans* embryo without requiring gene transcription in the responding cell. *Genes Dev.* **13**, 2028–2038.
- Serpinskaya, A.S., Feng, G., Sanes, J.R., and Craig, A.M. (1999). Synapse formation by hippocampal neurons from agrin-deficient mice. *Dev. Biol.* **205**, 65–78.
- Serra-Pagés, C., Medley, Q.G., Tang, M., Hart, A., and Streuli, M. (1995). Liprins, a family of LAR transmembrane protein-tyrosine phosphatase-interacting proteins. *J. Biol. Chem.* **273**, 15611–15620.
- Shapiro, L., and Colman, D.R. (1999). The diversity of cadherins and implications for a synaptic adhesive code in the CNS. *Neuron* **23**, 427–430.
- Shulman, J.M., Benton, R., and St. Johnston, D. (2000). The *Drosophila* homolog of *C. elegans* PAR-1 organizes the oocyte cytoskeleton and directs oskar mRNA localization to the posterior pole. *Cell* **101**, 377–388.
- Suter, D.M., and Forscher, P. (1998). An emerging link between cytoskeletal dynamics and cell adhesion molecules in growth cone guidance. *Curr. Opin. Neurobiol.* **8**, 106–116.
- Thompson, J.D., Higgins, D.G., and Gibson, T.J. (1994). CLUSTAL W: improving the sensitivity of progressive multiple sequence alignment through sequence weighting, position-specific gap penalties and weight matrix choice. *Nucleic Acids Res.* **22**, 4673–4680.
- tom Dieck, S., Sanmarti-Vila, L., Langnaese, K., Richter, K., Kindler, S., Soyke, A., Wex, H., Smalla, K.H., Kampf, U., Franzer, J.T., et al. (1998). Bassoon, a novel zinc-finger CAG/glutamine-repeat protein selectively localized at the active zone of presynaptic nerve terminals. *J. Cell Biol.* **142**, 499–509.
- Troemel, E.R., Sagasti, A., and Bargmann, C.I. (1999). Lateral signaling mediated by axon contact and calcium entry regulates asymmetric odorant receptor expression in *C. elegans*. *Cell* **99**, 387–398.
- Wan, H.I., DiAntonio, A., Fetter, R.D., Bergstrom, K., Strauss, R., and Goodman, C.S. (2000). Highwire regulates synaptic growth in *Drosophila*. *Neuron* **26**, 313–329.
- White, J.G., Southgate, E., Thomson, J.N., and Brenner, S. (1986). The structure of the nervous system of the nematode *C. elegans*. *Philos. Trans. R. Soc. Lond. B. Biol. Sci.* **314B**, 1–340.
- Williams, B.D. (1995). Genetic mapping with polymorphic sequence-tagged sites. *Methods Cell. Biol.* **48**, 31–58.
- Zhen, M., and Jin, Y. (1999). The liprin protein SYD-2 regulates the differentiation of presynaptic termini in *C. elegans*. *Nature* **401**, 371–375.
- Zhen, M., Xun, H., Bamber, B., and Jin, Y. (2000). Regulation of presynaptic terminal organization by *C. elegans* RPM-1, a putative GTP-GDP exchanger with a Ring-H2 finger domain. *Neuron* **26**, 331–343.